

Particle tracking

Valerio Vagelli

Italian Space Agency – Science and Research Directorate

06 June 2022 – 10 June 2022

For any questions, doubts and critics
valerio.vagelli@asi.it

Disclaimer:

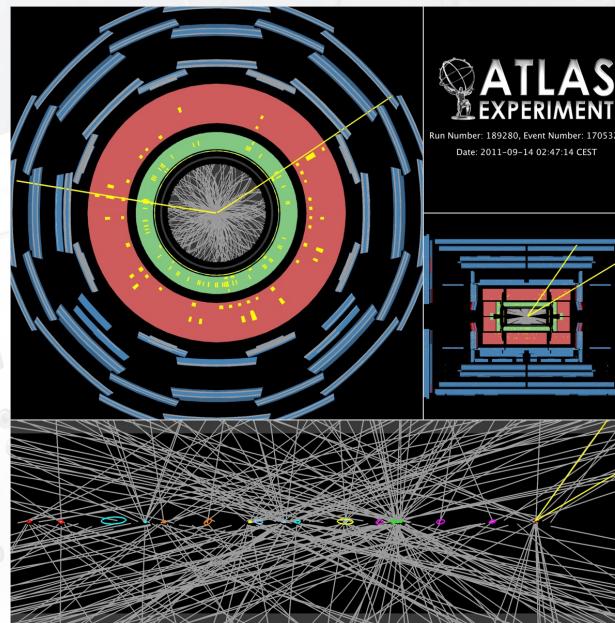
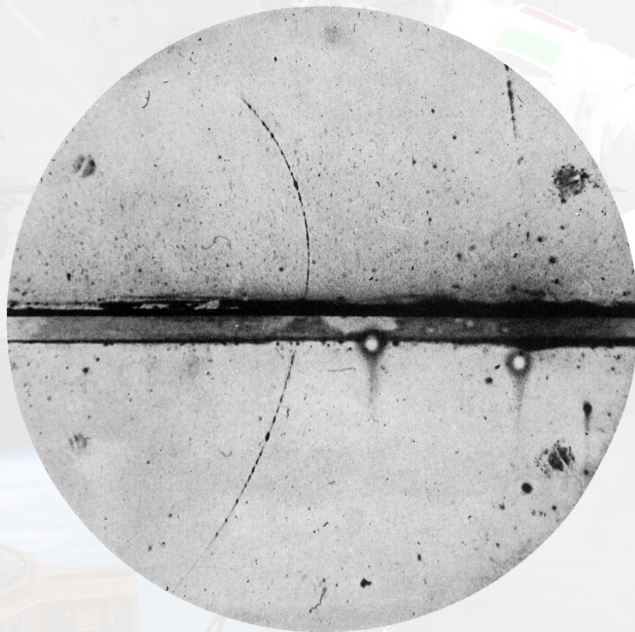
Huge field of technological solutions, applications, data analysis approaches

I will cover only a selection of topics and applications, mostly what I have
experience with

(Please apologize if your favourite detector is not covered...)

Track visualization in HEP

Track **visualization** to identify: particle trajectories, particle decays points, interaction vertex



Full digital readout → reconstruction of particle trajectories using few sampling points
Minimal disruption of particle properties (see calorimeters)

Particle Identification

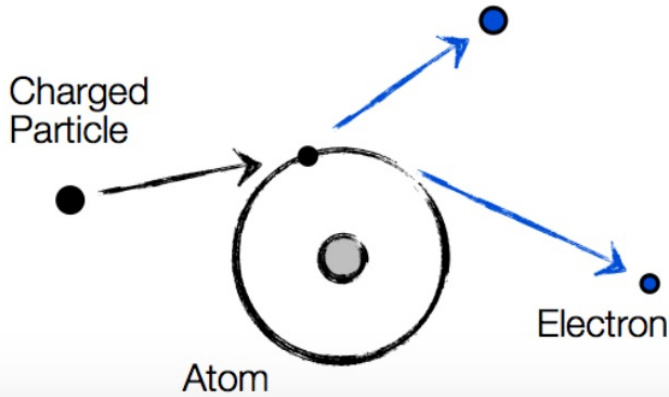
- Particles are uniquely identified by their **velocity**, **momentum** and **sign of the charge** combining the information from several subdetectors
- Curvature in magnetic field $\rho \propto R = \frac{p}{Ze}$
- Velocity after time of flight measurements $\beta \propto \frac{1}{\Delta T}$
- Ionization losses $\frac{dE}{dX} = f(z, \beta)$
- Calorimetric measurements $E_{kin} = (\gamma - 1)mc^2$
- Typically, measurements are more than the number of searched parameters → **multiple measurements used to over-constrain the values and to crosscheck systematic effects**
- NB: at high energies ($\beta \rightarrow 1$), the sensitivity of velocity measurements decreases. Complementary techniques used to infer the particle energy.



Ionization energy losses

Main effect of energy loss in materials: **continuous energy losses by ionization from scattering off atomic electrons**

Scattering off electrons: high energy losses, small trajectory deviation
 Scattering off nuclei: small energy losses, high scattering angles (multiple scattering)

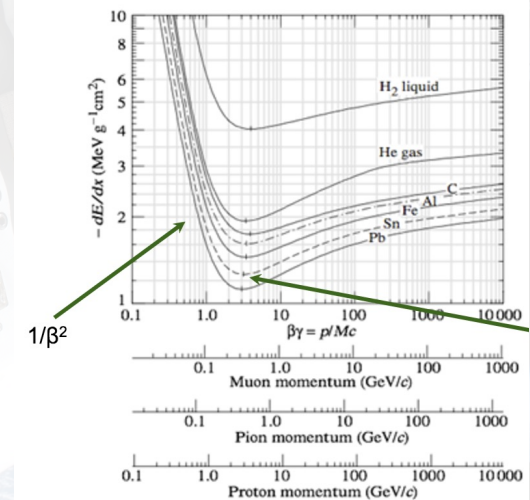


Bethe-Block formula: energy loss per unit of grammage $X = \rho x$

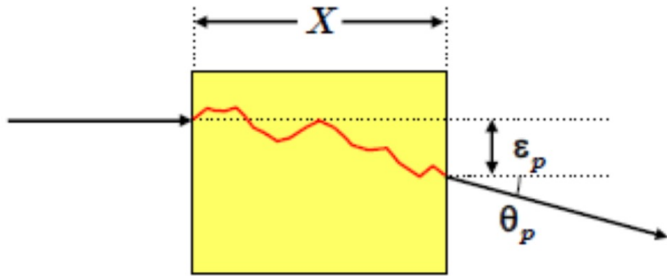
$$\frac{dE}{dX} = 0.31 \text{ MeV}/(\text{g}/\text{cm}^2) z^2 \frac{Z}{A} \frac{1}{\beta^2} \left[\frac{1}{2} \log(f(\beta)) - \beta^2 - \delta(\beta\gamma) \right]$$

Energy loss depends on particle and medium properties.

$\frac{dE}{dX} \propto z^2$ **proportionality to particle charge used to identify heavy nuclei**



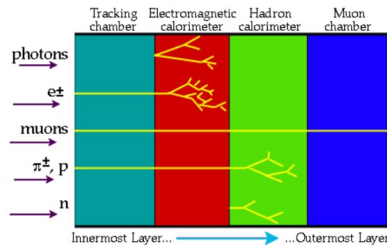
Coulomb Multiple Scattering



Particles moving through the detector material suffer many e.m. interactions that randomly deviate their trajectory (stochastic process)

After crossing material with depth X , the particle trajectory undergoes:

- an angular deviation
- a trajectory offset (often negligible in thin detectors)

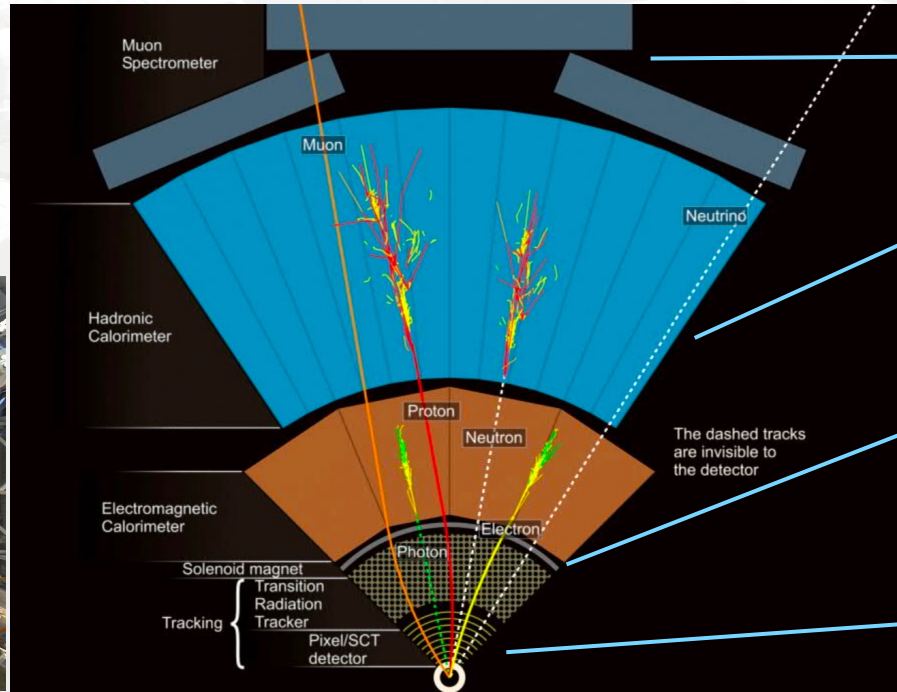
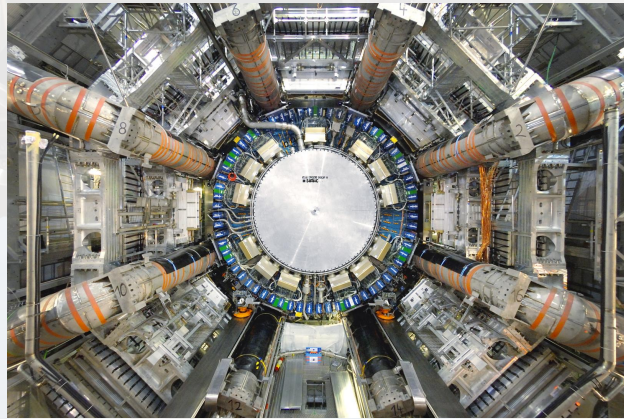


$$\theta_{RMS} = \frac{13.6 \text{ MeV}}{\beta c p} \approx \sqrt{X/X_0} (1 + 0.038 \ln(X/X_0))$$

At low momentum, position and momentum resolution are dominated by multiple scattering

A typical collider particle detector

ATLAS @ LHC



Measurement of muons
crossing calorimeters
($> 2-3 \text{ GeV}$)

Charged hadron absorption
Neutral hadron detection
 $5-6\lambda_1$

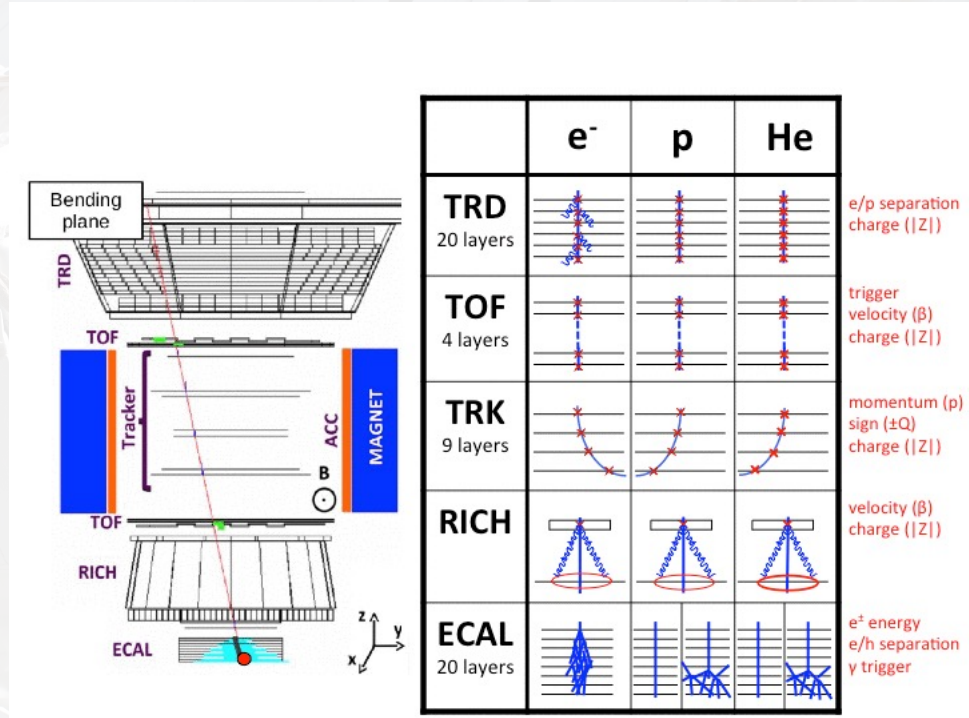
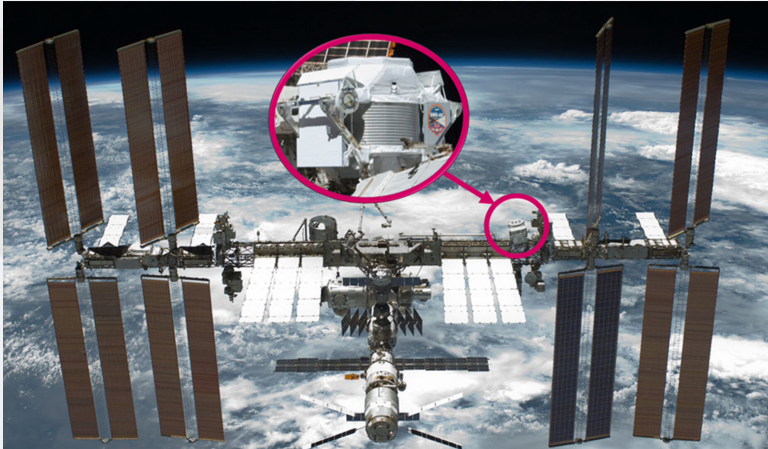
Electron identification
Photon detection
($\sim 20X_0, 1-2\lambda_1$)

Momentum measurement
decay vertex recon.
Hadron identification
Low material ($\leq 1X_0$)

The dashed tracks
are invisible to
the detector

A typical space particle detector

AMS @ ISS



Tracker goals

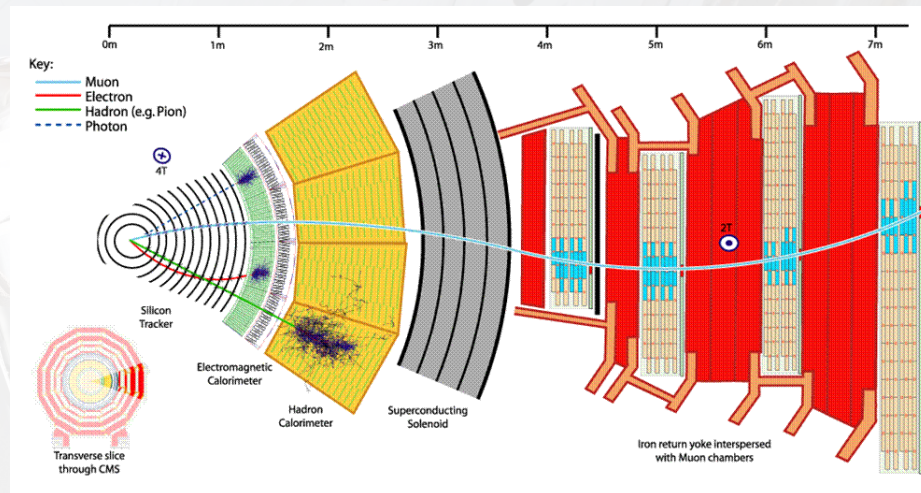
"Particle flow" @ CMS

Reconstruct charged-particle trajectories

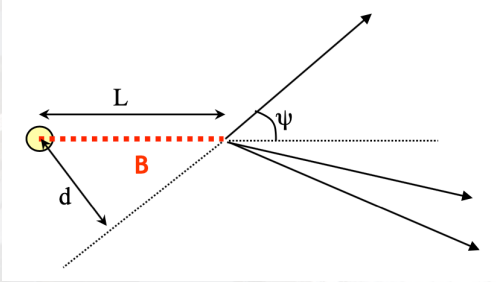
- join seed points to create a track ("pattern recognition")
- measure **direction** and **position**
- measure **momentum** and **charge** (with magnetic field)
- two major configurations in colliders: **inner spectrometers** and **external muon systems**

Reconstruct decay and interaction vertices

- primary vertex: collision point
- secondary vertex: decay of unstable particle or interaction with detector material



Vertex detectors



$$d = L \sin\psi = O(\gamma\beta c\tau) \cdot O(\gamma^{-1}) = O(c\tau)$$

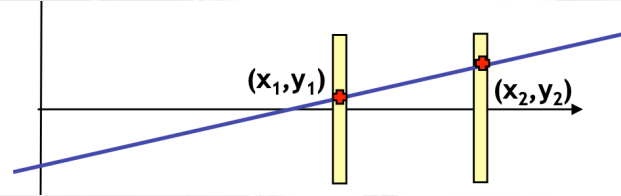
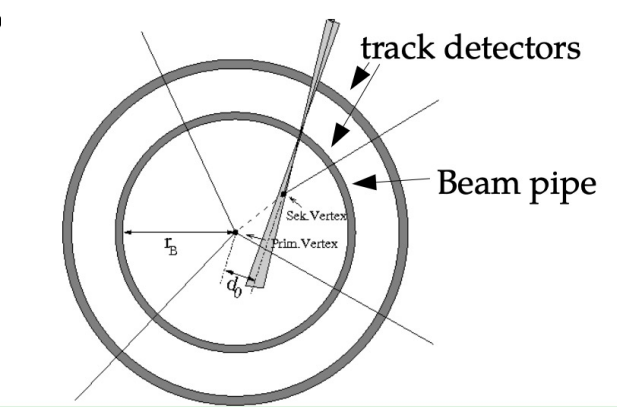
NB: mostly independent on boost for ultrarel. particles

impact parameter d , defined as the distance between the daughter particle trajectory and the mother particle production point

Vertex detectors measure the primary interaction vertex and secondary vertices from secondary decays

An experimental apparatus with decay vertex capabilities must be able to separate the production and decay vertices: $\sigma(L) / L \ll 1$

Uncertainty in d depends on detector radii and coordinate resolution



$$\sigma_d^2 = \frac{(r_2\sigma_1)^2 + (r_1\sigma_2)^2}{(r_2 - r_1)^2} + \sigma_{MS}^2$$

Small σ_1 and σ_2 : precision coordinate measurement

Small r_1 , large r_2

Measurement is degraded by multiple scattering in materials

Tracker technologies

Gaseous detectors

- Based on ionization in gas
- Requires gas amplification $O(10^4)$ or more) to achieve enough S/N

Not covered

Silicon detectors

- based on creation of e/h pair carriers in semiconductor material
- no amplification is needed (~ 100 carriers/ μm)

Fiber trackers

- Based on light readout from scintillating fibers
- scintillation light materials with photodetectors sensitive to single electrons

Slightly covered

Silicon sensors



Monocrystalline silicon lingot
(@SUMCO)



Silicon wafer substrate
(@Mi-NET)

(At this stage mostly all detectors look the same)

Moderate energy gap band

$$E_g = 1.12 \text{ eV} \Rightarrow E(\text{e-h pair}) = 3.6 \text{ eV}$$

$\approx 30 \text{ eV}$ for e-ion in gas detectors, $\approx 100 \text{ eV}$ for photon in scintillators

- High carrier yield
- Improved energy resolution and high signal

High density

$\sim 2.33 \text{ g/cm}^3 \rightarrow$ High specific energy loss

dE/dX (M.I.P.) $\approx 3.8 \text{ MeV/cm}$, $\approx 100 \text{ e-h}/\mu\text{m}$ (average)

- Thin detectors
- Reduced range of secondary particles
- Better spatial resolution

High carrier mobility

$\mu_e = 1450 \text{ cm}^2/\text{Vs}$, $\mu_h = 450 \text{ cm}^2/\text{Vs}$ fast charge collection ($< 10 \text{ ns}$)

Excellent physical properties

- Can be produced with high purity
- Rigid, allows the use of self-supporting structures
- Industrial technology, relatively low price, small structures workable
- High intrinsic radiation hardness

Position sensitive Silicon sensors

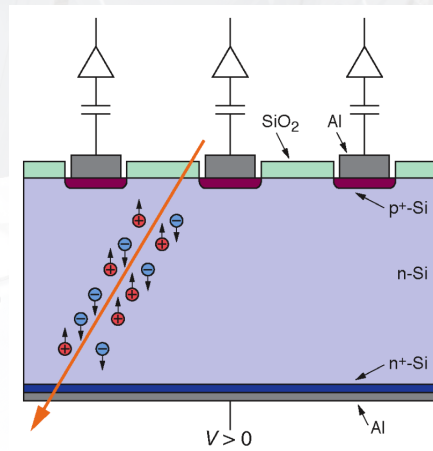
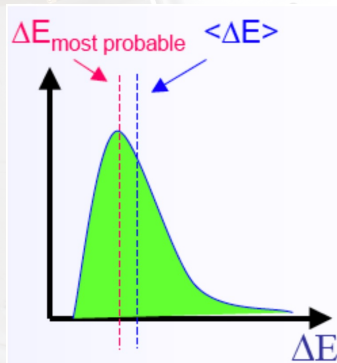
Segmentation of one surface in sensitive elements
strips, pads, pixels

Typical parameters

- Thickness 150 μm – 500 μm
- Pitch (strip separation): 25 μm – 150 μm
- Coordinate resolution down to few μm
- Charge collection O(10ns)
- Charge integration O(100ns)
- Operation voltage < 200V

Signal output

- Average energy loss of MIP in Si
3.6 eV/pair, ~ 80 pairs/ μm (MP)
- 300 μm thickness : O(25k) pairs/MIP
- Charge: O(5fC)



Simple layout DC-coupled



Landau energy distribution in thin sensors

Asymmetric probability function with a long “tail” due to large energy deposits

applies in thin O(100 μm) Si sensors

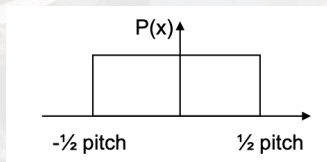
Most probable: ≈ 80 e-h⁺ pairs per μm
Average value: ≈ 100 e-h⁺ pairs per μm

NB: Bethe Block describes $\langle \Delta E \rangle$

Intrinsic resolution

Position measurement comes from segmentation / pitch

Digital resolution:



Position = strip center
Resolution: $p/\sqrt{12}$

Improvement from **signal sharing**:

Assuming signal amplitude prop. to deposited energy

- requires analog signal readout

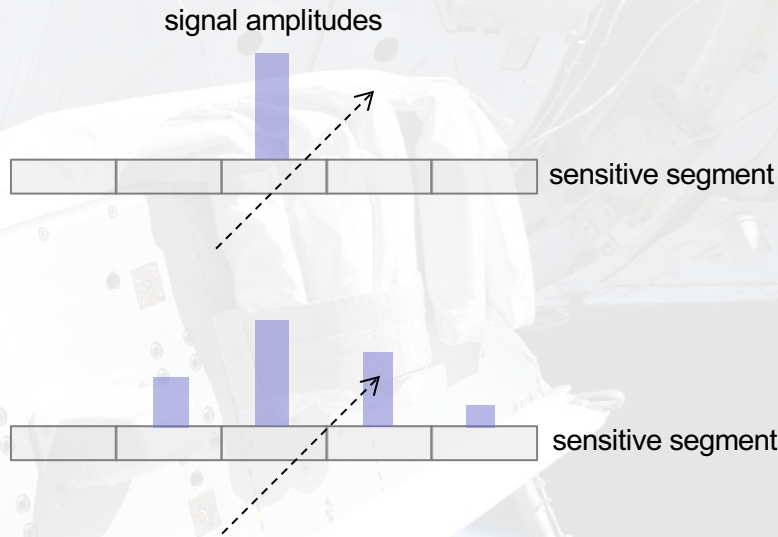
Position = charge center of gravity

Hits are defined as segments with S/N above threshold

Additional hits generated by:

- secondary charge spread inside the sensor volume
- inclined tracks

Signal sharing allows to achieve improved performances after proper calibration



Double-sided silicon sensors

Single sided sensors measure one coordinate only

- use stacks with strips running in different directions to achieve 3D trajectory reconstruction

Double sided sensors measure two coordinates in one layer

- backside implants run perpendicular to top strips

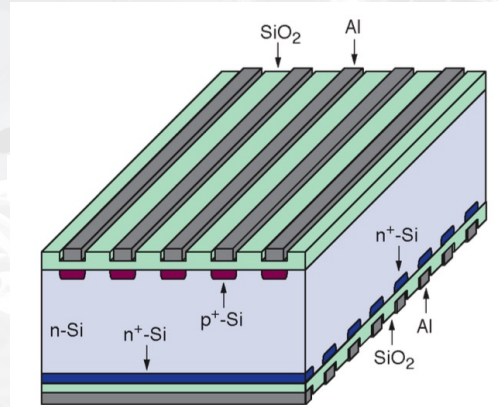
Pros:

- minimize material to measure 3D point in space

Cons:

- Production and handling is more complicated
- Test stations require peculiar modifications
- More expensive

Readout requires dedicated layouts to host FEE on one side only



Scheme of a double-sided microstrip detector (biasing structures not shown):

Holes drift towards p⁺ strips

Electrons drift towards n⁺ strips



Pixel silicon sensors

Double sided silicon detectors measure 2D coordinate XY for single tracks crossing the sensor

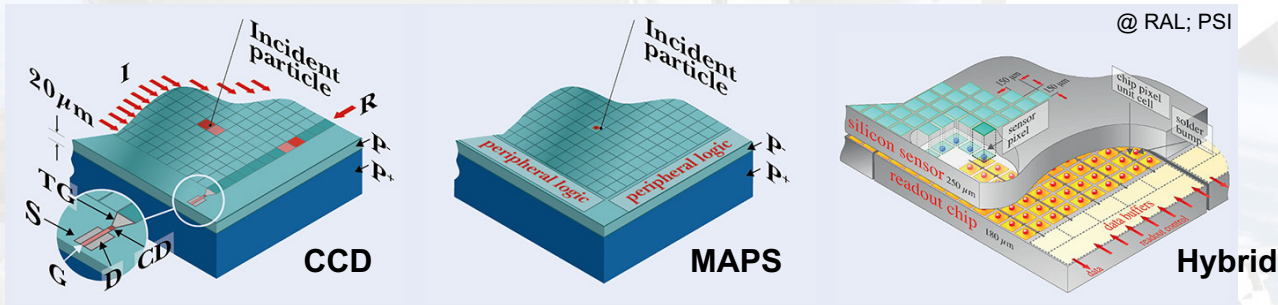
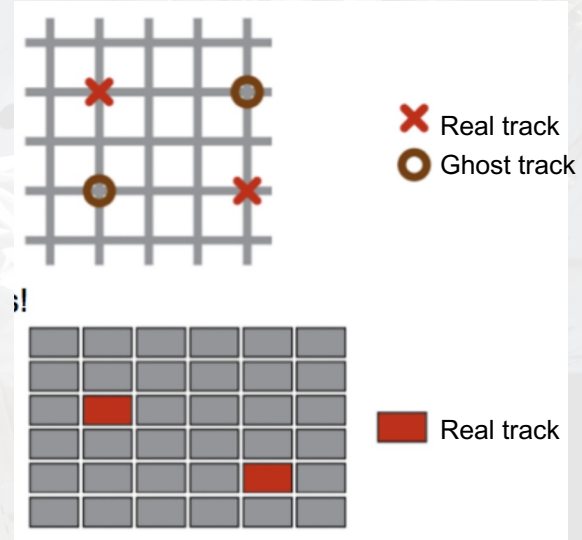
If additional particles cross the sensor during the detector integration time (i.e. "pileup"), we get ambiguity in hit association: "ghost hits"

For N crossing particles

- N^2 combinations
- $N^2 - N$ ghost hits

Peculiar strip geometries may mitigate the problem.

Pixel sensors completely tackle this issue



Pixel silicon sensors

Pixel size $O(50\mu\text{m} \times 50\mu\text{m})$ or less

If signal amplitude is not recorded (digital readout) resolution $p/\sqrt{12} \sim O(10\text{-}5 \mu\text{m})$

Pros:

- Small pixel area:
 - √ low detector capacitance $O(1\text{fC} / \text{pixel})$
 - √ large S/N > 100
- Small pixel volume:
 - √ low leakage current $O(1\text{pA} / \text{pixel})$

Cons:

- Large number of readout channels per covered area
- Large number of electrical connections per covered area
- Large power consumption per covered area
- Unaffordable with standard bonding approaches



Half of the SLD vertex detector, consisting of 307 Mpixels, three barrels and a pixel size of $20 \times 20 \times 20 \mu\text{m}^3$. Each ladder of 16 cm active length contains two 8 cm-long stitched CCDs

Silicon sensor technology

Strip and hybrid pixel detectors are mature technologies employed in almost every experiment in high energy physics

Additional interesting silicon detector structures are:

Silicon Drift Detectors (SDD)

Monolithic Active Pixels (MAPS)

3D detectors

Charged Coupled Devices (CCD)

Depleted Field Effect detectors (DEPFET)

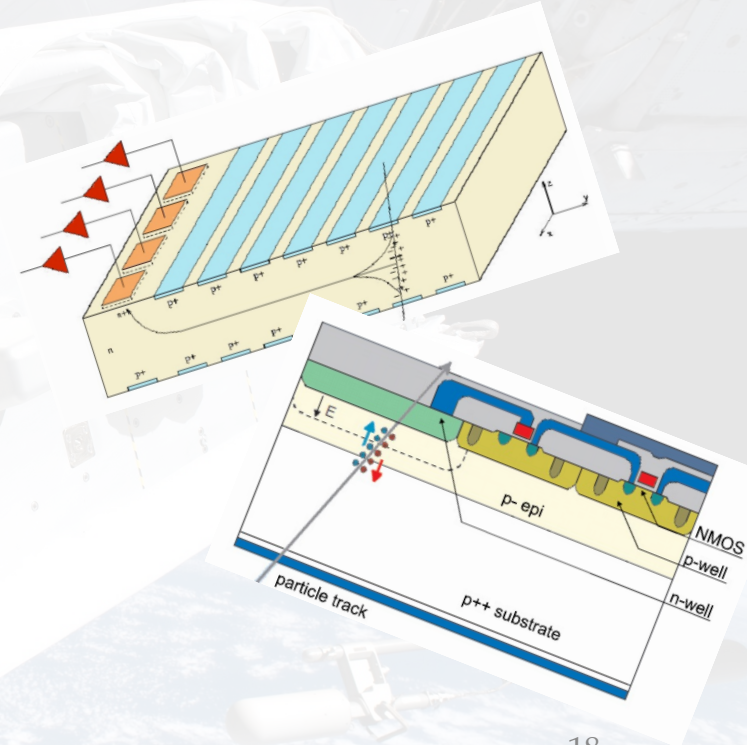
Silicon On Oxide (SOI)

Avalanche Photo Diodes (APD) and Silicon Photo Multiplier (SiPM)

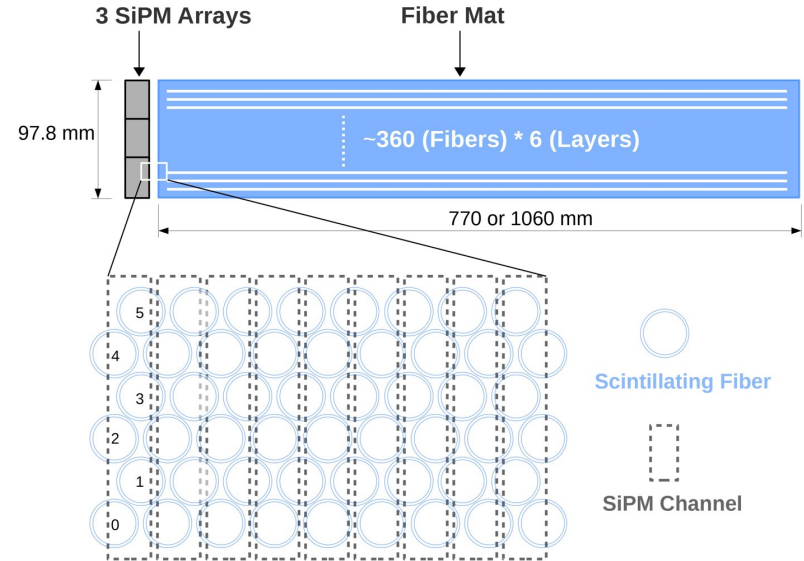
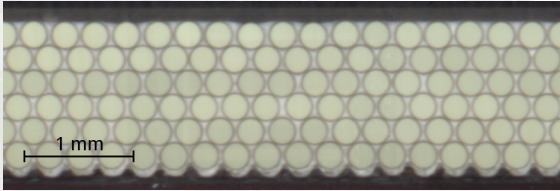
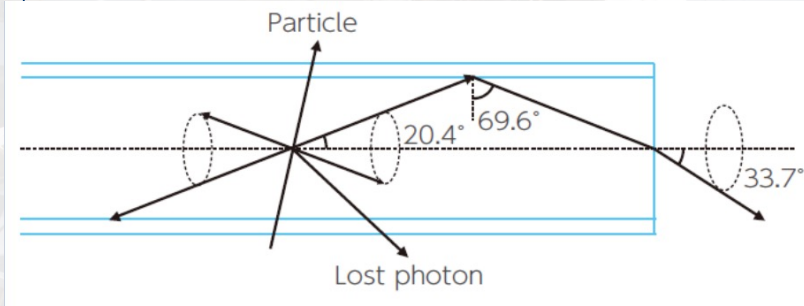
Time performant Si detectors:

Low Gain Avalanche Diodes / Ultra Fast Silicon Detectors

may enable "4D tracking" with Si-detectors with timing performances < 100 ps



Fiber trackers

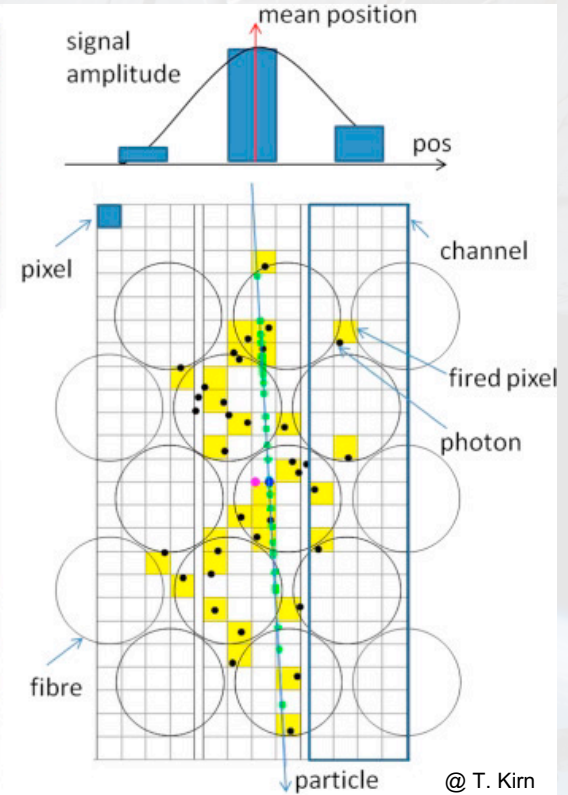
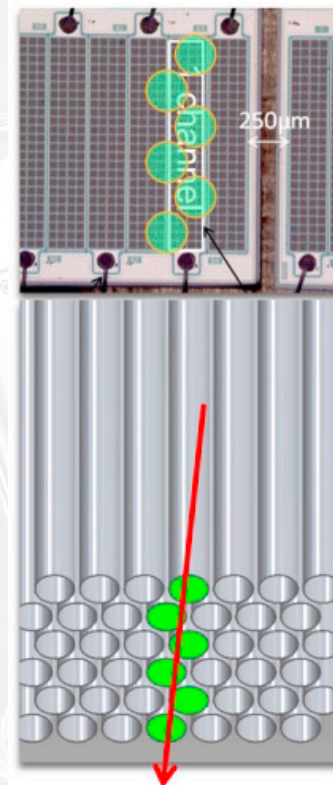
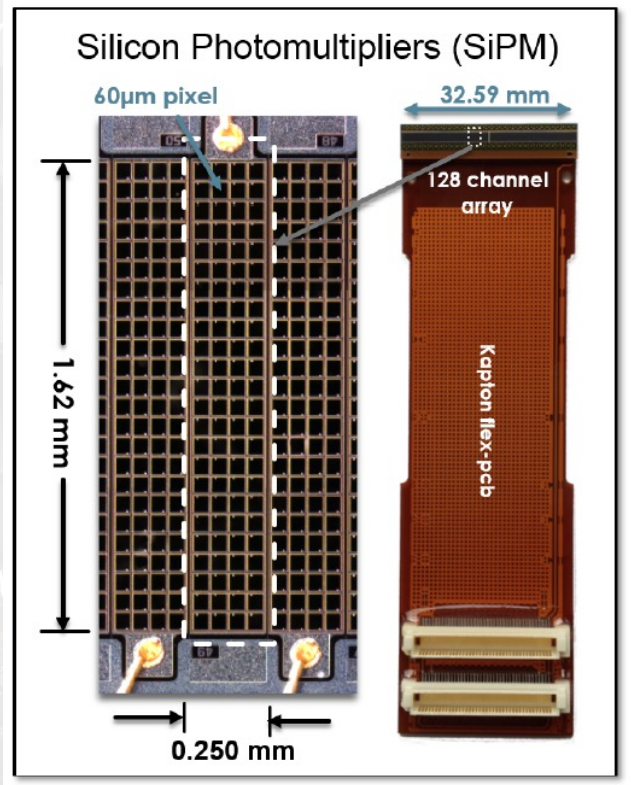


Alternative technology for charge particle tracking based on **SiPM + fiber-bundle coupling**.

- Cheaper cost/area than Si- μ strip
- Mechanical flexibility and adaptability
- Fibers can be up to 2m long without significant light absorption.
- Spatial resolution \sim determined by fiber pitch (with small improvements by SiPM pitch and fiber cross-correlations)

Fiber trackers

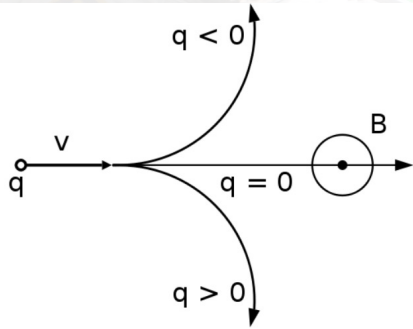
The Sci-Fi tracker for the LHCb detector upgrade



@ T. Kim

Momentum measurement

Determination of momentum of charged particles by measurement of the bending of a particle track/trajectory inside a magnetic field volume



$$\vec{F} = q\vec{v} \times \vec{B}$$

Lorentz force: is the force on a point charge due to electromagnetic fields

$$\frac{mv^2}{r} = qvB$$

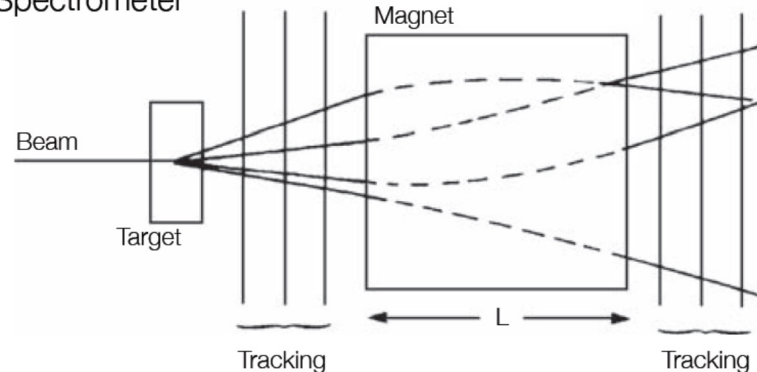
... for a particle in motion perpendicular to a constant B field

In practice:

- use layers of position sensitive detectors before and after (or inside) a magnetic field to measure a trajectory
- determine the bending radius

$$\rho \propto R = \frac{p}{Ze}$$

Schematics of a Spectrometer



@ E. Garutti

Momentum measurement: fixed target

Momentum determination
in fixed target experiments ...

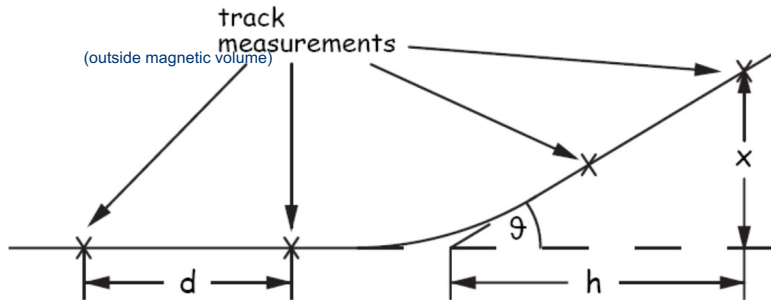
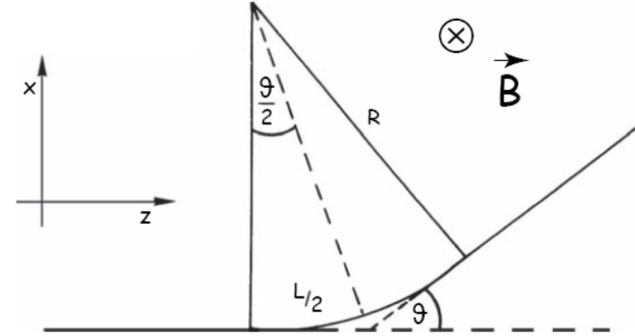
$$p = eRB \quad \vartheta = L/R$$

$$= L/p \cdot eB$$

$$p = eB \cdot L/\vartheta$$

Momentum
resolution:

$$\rightarrow \frac{\sigma_p}{p} = \frac{\sigma_\vartheta}{\vartheta} \quad \text{with} \quad \sigma_\vartheta \sim \sigma_x$$



Determination
of σ_p/p :

$$\vartheta = \frac{x}{h} \quad \sigma_\vartheta = \frac{\sigma_x}{h}$$

$$\frac{\sigma_p}{p} = \frac{\sigma_\vartheta}{\vartheta} = \frac{\sigma_x}{h} \cdot \frac{p}{eBL}$$

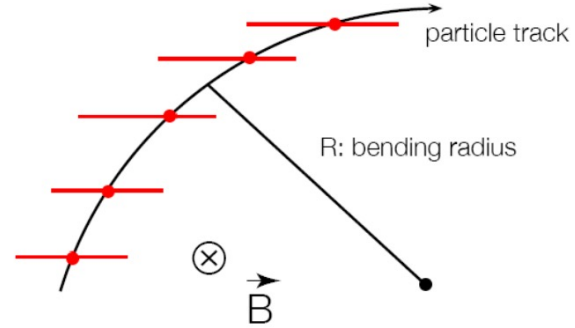
Long lever arm improves
momentum resolution ...

Momentum meas. in magnetic volume

Momentum determination
in a cylindrical drift chamber ...

$$\frac{mv^2}{R} = evB \quad \rightarrow \quad p = eB \cdot R$$

$$p \left[\frac{\text{GeV}}{c} \right] = 0.3 \text{ B[T]} R[\text{m}]$$



momentum component perpendicular to the B-field
transverse momentum p_t

For Sagitta s :

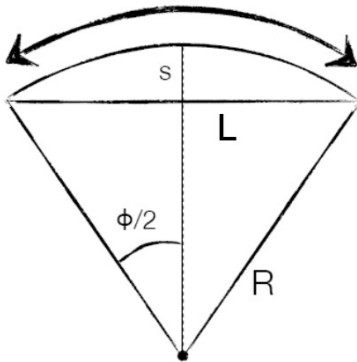
$$s = R - R \cos \frac{\phi}{2} \approx R \frac{\phi^2}{8}$$

$$s = R \frac{L^2}{8R^2} = \frac{L^2}{8R} \quad \text{and} \quad R = \frac{L^2}{8s}$$

$$\rightarrow \frac{\Delta p}{p} = \frac{\Delta R}{R} = \frac{L^2}{8Rs} \cdot \frac{\Delta s}{s}$$

$$\text{with } \phi = \frac{L}{R}$$

→ radius is obtained by a
circle fit through
measurement points along
the track with point
resolution σ_{rp}

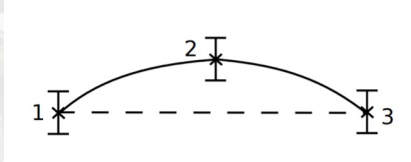


Momentum meas. in magnetic volume

Agenzia Spaziale Italiana

$$p = 0.3 B R \quad s = \frac{L^2}{8R}$$

$$\frac{\sigma(p)}{p} = \frac{L^2}{8Rs} \cdot \frac{\sigma(s)}{s} = \frac{8R}{L^2} \cdot \sigma(s) = \frac{8p}{0.3 B L^2} \cdot \sigma(s)$$



$$s = \frac{x_1 + x_2}{2} + x_3 \quad \sigma^2(s) = \frac{3}{2} \sigma^2(x)$$

$$\frac{\sigma(p)}{p} = \sqrt{\frac{3}{2}} \frac{8 \sigma(x)}{0.3 B L^2} \cdot p$$

For N equidistant samplings:

$$\frac{\sigma(p)}{p} \approx \sqrt{\frac{720}{N+4}} \frac{\sigma(x)}{0.3 B L^2} \cdot p$$

$$\frac{\sigma(p)}{p} \propto p, \sigma(x), \frac{1}{B L^2} \quad \mathbf{BL^2: Bending Power}$$

Spectrometer resolution worsens at high rigidities and can be improved with better coordinate measurement resolution and better bending power

- **L** ~ spectrometer dimensions, limited by space/mechanical constraints
- **B** limited by magnet size and technology (e.g., superconducting magnets in space)
- **$\sigma(x)$** position resolution, can be improved to resolutions depending on the application. Typically O(10 μ m)

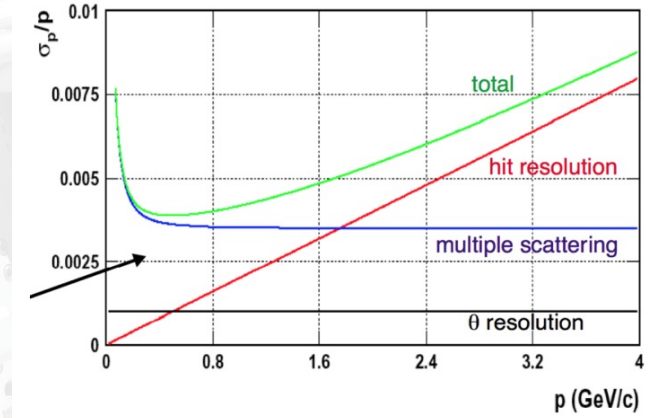
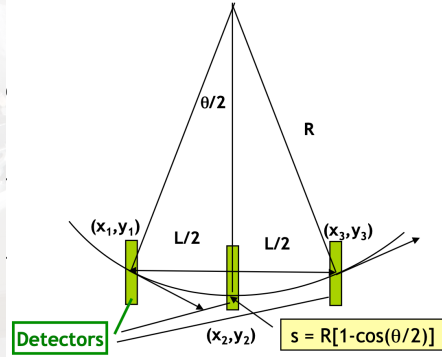
Multiple Scattering effects

Sensors provide material budget to particle crossing that results in deflection of the trajectory



$$\sigma^{MS}(s) \approx L^* \frac{1}{p\beta} \sqrt{L^*}$$

$$\frac{\sigma(p_T)}{p_T} = \frac{\sigma^{MS}(s)}{s} \approx \frac{\sqrt{L^*} L^* / (p\beta)}{0.3 B L^2 / p_T}$$



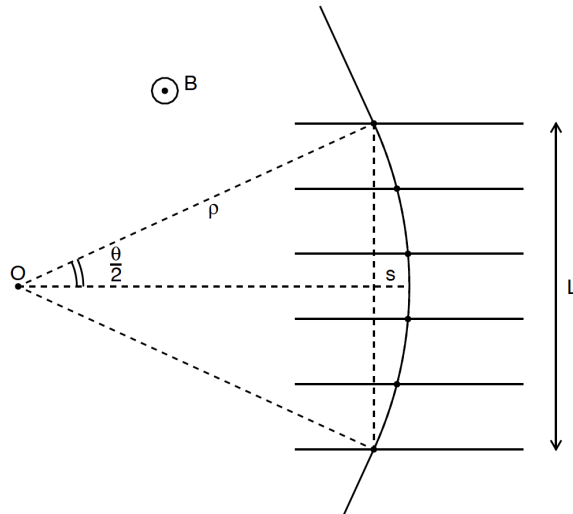
$$\frac{\sigma(p)}{p} \approx \sqrt{\frac{720}{N+4} \frac{\sigma(x)}{0.3 B L^2}} \cdot p \sin\theta \oplus \frac{0.2}{\beta B \sqrt{L X_0} \sin\theta}$$

Low energy momentum resolution is dominated by multiple scattering effects
When $\beta < 1$ more complicated effects enter in

Spectrometers

Magnetic Spectrometers

Simple 2D sagitta model



- Charged particle bent in magnetic field
- The sagitta is measured by sampling the particle trajectory through different planes
- The particle rigidity is inferred via

$$R(GV/c) = \frac{0.3 B(T) L(m)^2}{8 s(m)}$$

- Rigidity resolution scale linearly as

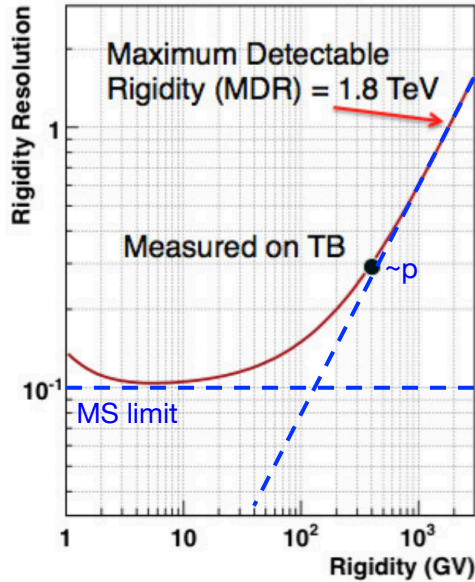
$$\frac{\sigma_R}{R} = \frac{\sigma_s}{s} \propto R$$

- Maximum Detectable Rigidity MDR

$$\frac{\sigma_R}{R} = 1 \Rightarrow R^{(MDR)} \propto \frac{L^2 B}{\sigma_s}$$

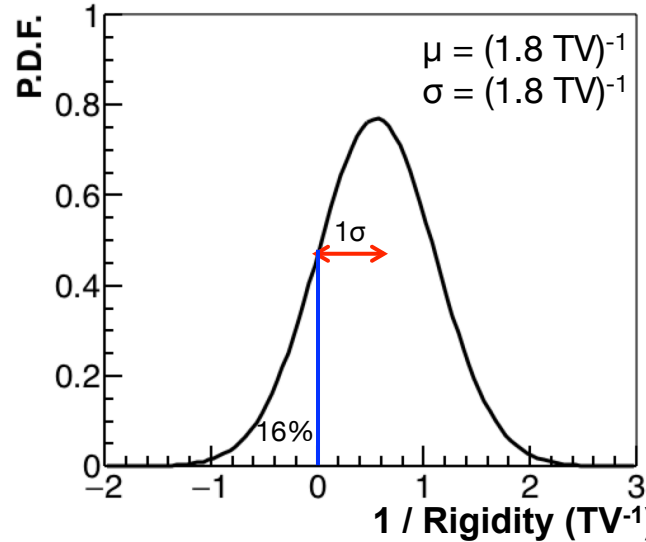
Figure of merit often used to compare spectrometer performances

Spectrometers



Performance parameter:
Maximum Detectable Rigidity (MDR):

$$\frac{\sigma_R}{R} = 1 \Rightarrow R^{(\text{MDR})} \propto \frac{L^2 B}{\sigma_s}$$



At high energies $\frac{\sigma(p)}{p} \propto p$

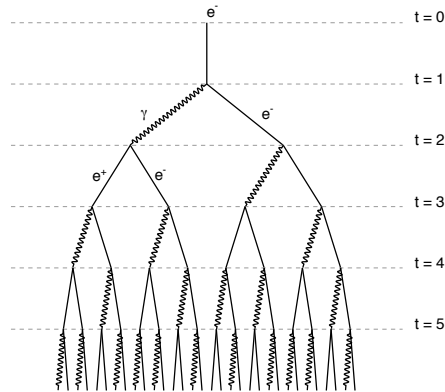
At low energies $\frac{\sigma(p)}{p} \approx \text{const}$
(Multiple scattering) p

“Spillover”: events that are reconstructed with opposite sign of charge

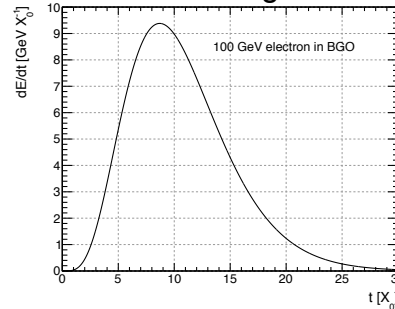
Calorimetry

Calorimeters

Simple electromagnetic shower profile



- Calorimeters measures the energy releases of the particle
 - Homogeneous / Sampling
 - Electromagnetic / Hadronic



$$\frac{dE}{dt} = E_0 b \frac{(bt)^{a-1} e^{-bt}}{\Gamma(a)}$$

- The energy resolution improves as the energy increases

$$\frac{\sigma_E}{E} = \frac{a}{\sqrt{E}} \oplus \frac{b}{E} \oplus c$$

Statistical fluctuations

Inhomogenities, calibration, energy leaks,...

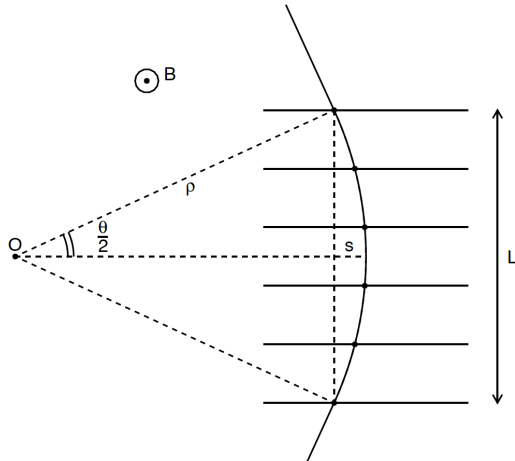
Electronics

BUT: energy resolution is not everything. Typically the dominant systematic is the knowledge of the energy scale!!

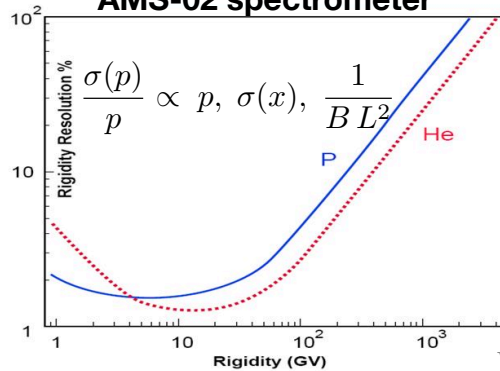
- Resolution \rightarrow Symmetric smearing of measured energy
- Energy scale \rightarrow Systematic shift of measured energy

Energy measurements

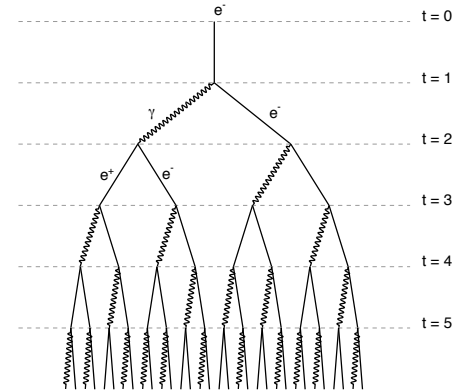
Magnetic Spectrometers



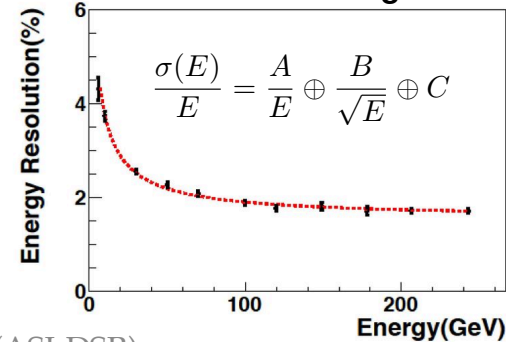
AMS-02 spectrometer



Calorimeters



AMS-02 electromagnetic calorimeter

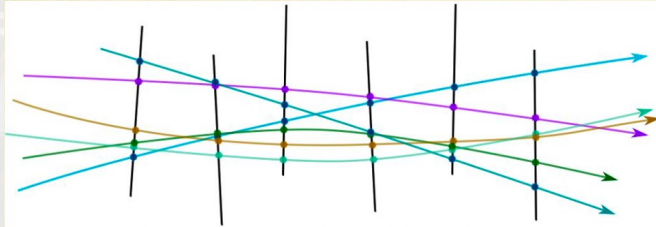


Tracker alignment

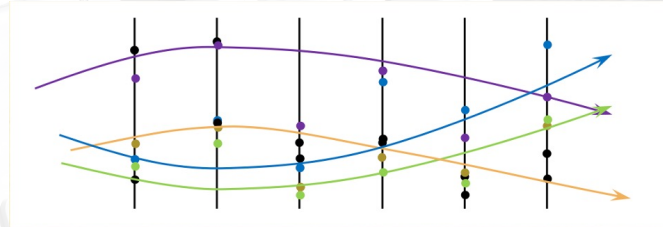
Implicit hypothesis: "We know the absolute coordinate of the track sampling"

Typically WRONG!

- Mechanical uncertainties and instabilities due to magnetic field, temperature etc...
- Drift speed variations (detector inhomogeneities)



True trajectories and True detector layout



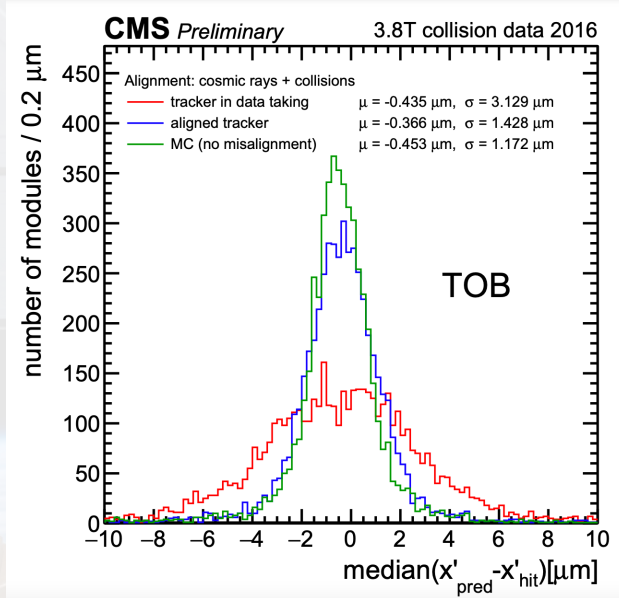
Detector layout assumptions and tracks built on this hypothesis

NB: relative point positions along the sensors are correct. Tracks are not.

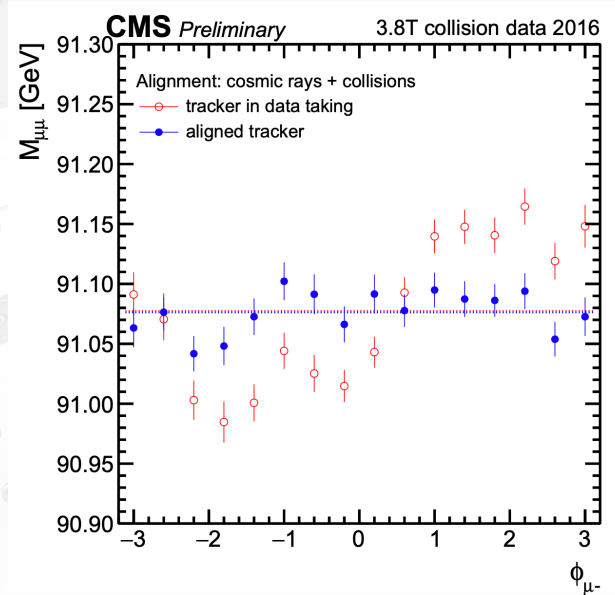
Solutions in detector design are useful to mitigate this effect. But offline analysis corrections are needed
"Alignment"

Tracker alignment

Example: effect of misalignment in CMS tracker systems

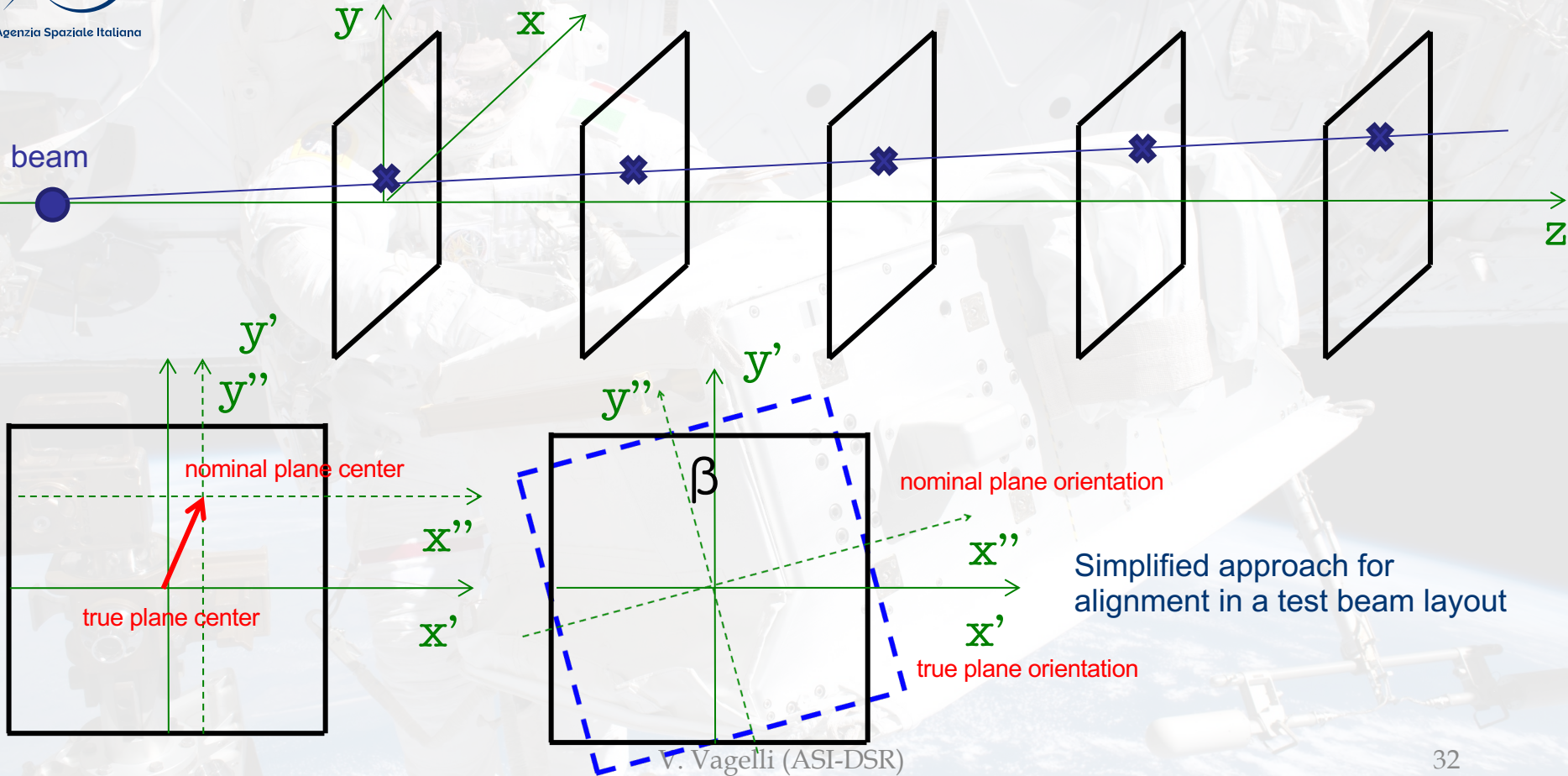


Distribution of median residuals for
tracker outer barrel



Reconstructed $Z \rightarrow \mu\mu$ as function
of Φ of μ^-

Simple tracker alignment at test beam



Tracker alignment

Alignment parameters:

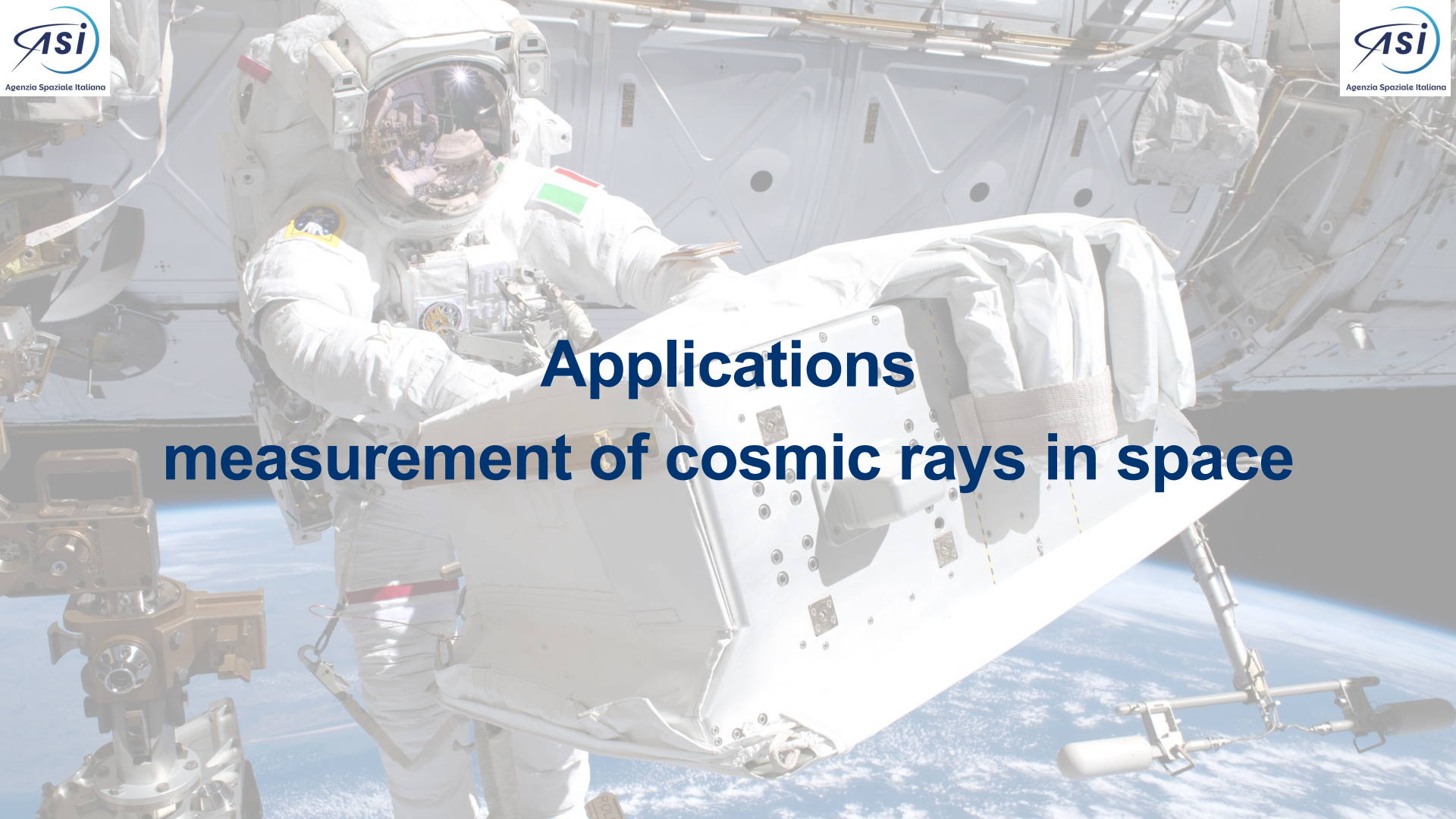
the track model depends on additional free factor, i.e. the sensor positions and orientations

Methods:

- **Global alignment:** fit all parameters to minimize the overall χ^2 of a set of tracks (Millipede algo.). Many parameters are involved.
- **Local alignment:** use tracks reconstructed with reference detectors or calibration lasers and align other detectors by using "reference" tracks and minimize the distribution of residuals (track-hit distance)

For all cases, use particle probes in simple data taking environments:

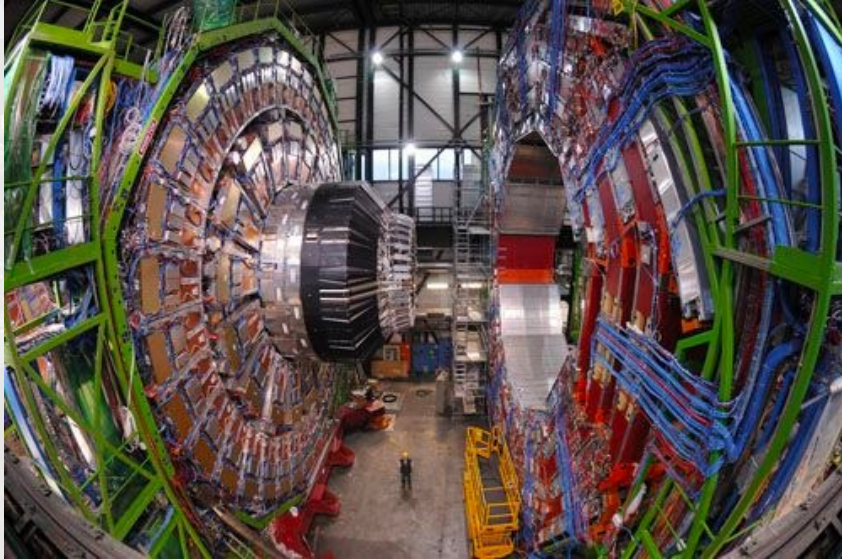
- low-multiplicity events
- Muons
- High energy particles (no trajectory bending in magnetic field)
- possibly no magnetic field



**Applications
measurement of cosmic rays in space**

Measurement of Cosmic Rays in Space

Particle physics detectors operated in the "laboratory" of space



CMS detector at LHC (CERN)

Source: particles accelerated in lab

Weight / Volume: 14'000 tons / 15 x 15 x 21 m²

Electronics channels: ~ 100 M

Magnetic field: 4 T

Power consumption: ~ 5 MW (only detector, no services)



AMS detector in space (ISS)

Source: particles accelerated in the Cosmos

Weight / Volume: 8 tons / 3 x 4 x 5 m²

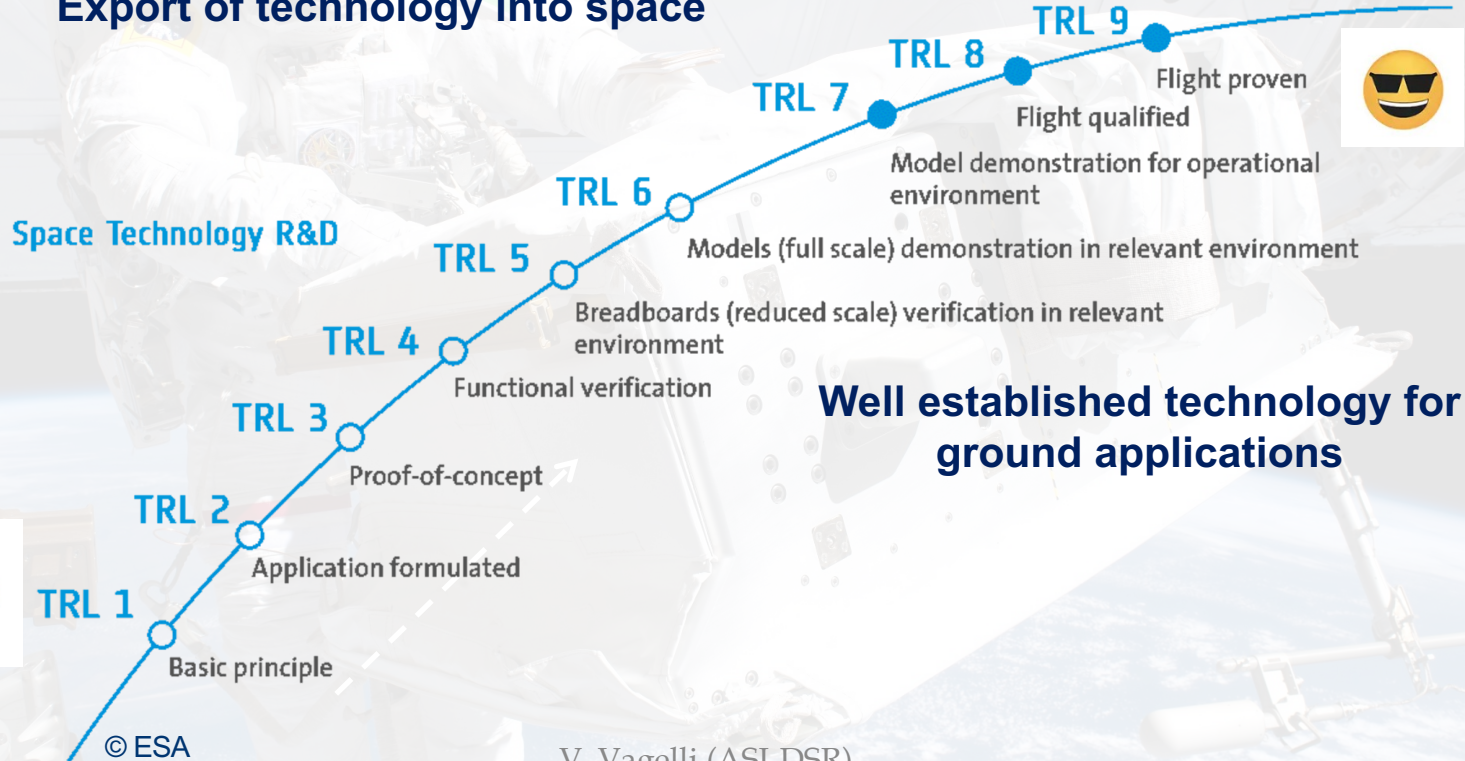
Electronics channels: ~ 300 k

Magnetic field: 0.14 T

Power consumption: ~ 2 kW (whole experiment)

Space technology development

Export of technology into space



Requirements of detectors in space

performance a la 'particle physics':

- high resolution measurements of momentum, velocity, charge and energy

characteristics to properly access and work in space:

- Vibration (6.8 G rms) and acceleration (17 G)
- Temperature variation (day/night $\Delta T = 100^{\circ}\text{C}$)
- Vacuum (10^{-10} Torr)
- Orbital debris and micrometeorites
- Radiation (Single Event Effect)

limitation in

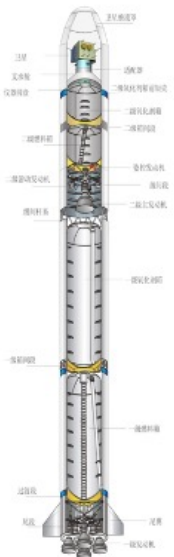
- weight O(tons)
- power (few kW), bandwidth and maintenance

Compliant with EMC (e.m. compatibility) specs



(all stress factors depend on the details of the mission. here AMS-02 reference values are reported)

Operations in space

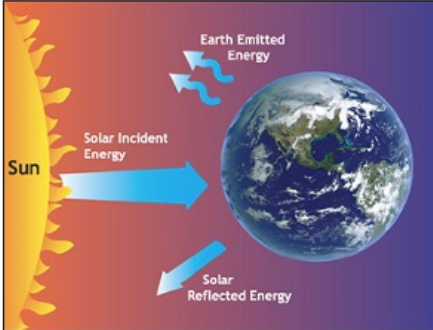


Mechanical stress at launch:

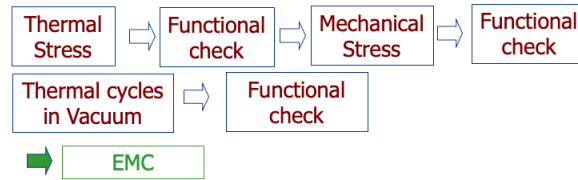
- Static acceleration
- Random vibration
- Sinusoidal vibration
- Pyroshock

Life in space:

- Thermal stresses due to Sun-light (seasonal / day-night effects)
- Vacuum



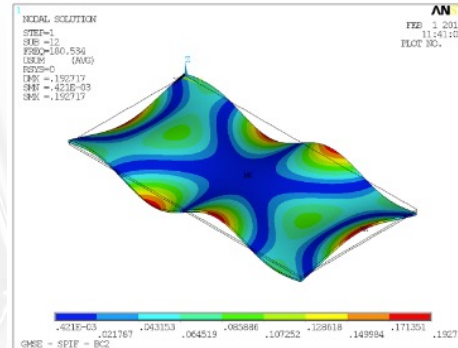
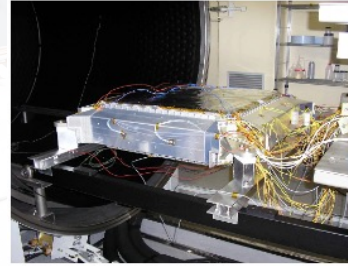
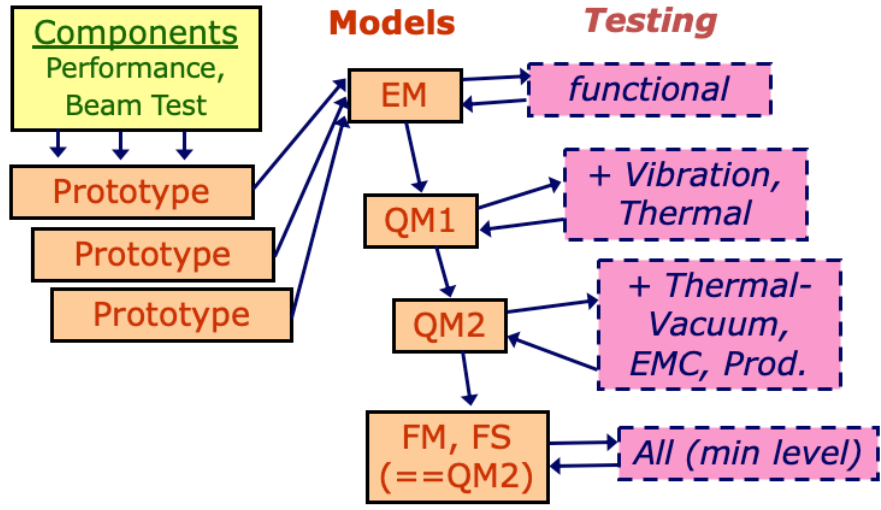
Careful Design, Model validation and Qualification are needed to ensure *highest possible reliability*



The long process to fly....

THERMO-VACUUM TESTS

VIBRATION TESTS



THERMAL MODELS

The extreme thermal environment

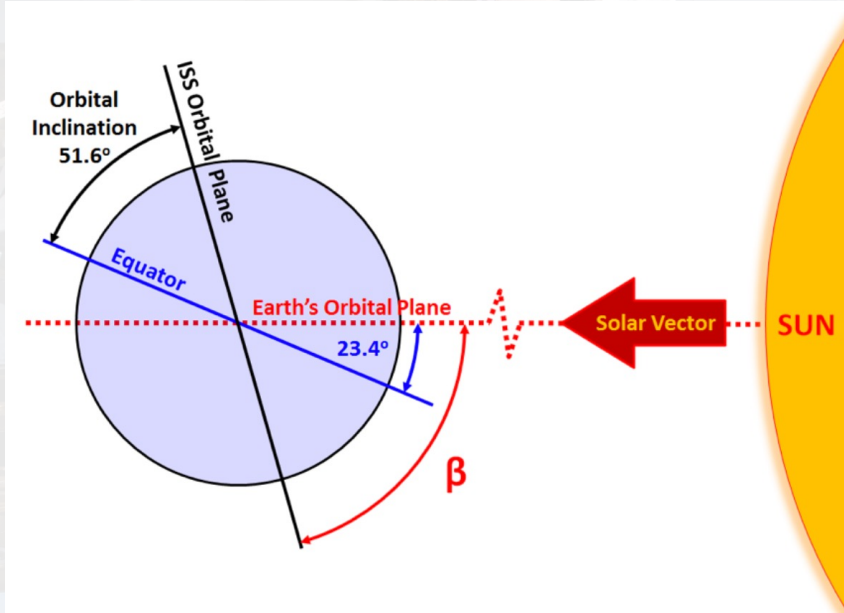


Figure 1. The solar beta angle, β , is the angle between the ISS orbital plane and the solar vector (direction from the Sun to the Earth).

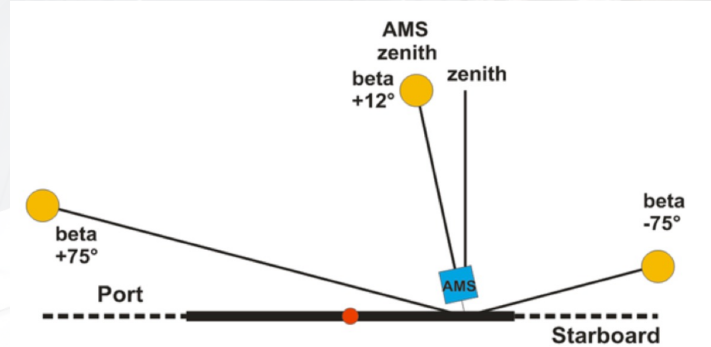


Figure 2. Variation of direction of solar illumination with beta angle. To avoid the rotating ISS solar arrays periodically being in its field of view, AMS is mounted on the ISS with a $+12^\circ$ "roll" to port.

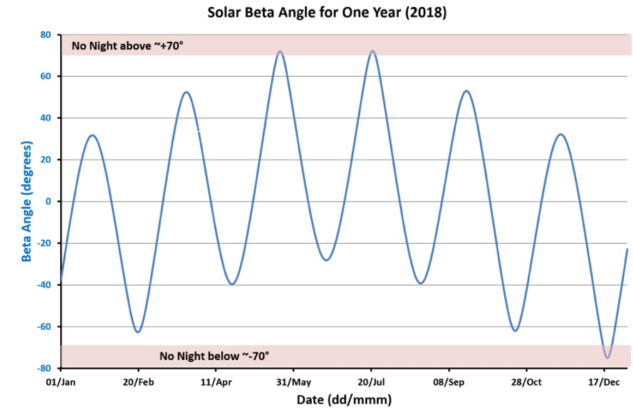


Figure 3. The solar beta angle for the year 2018. The shading indicated the times when there is no night on orbit.

Measurement of Cosmic Rays in Space



Long missions (years)
Small payloads
Low energies..

IMP series < GeV/n
 ACE-CRIS/SIS E_{kin} < GeV/n
 VOYAGER-HET/CRS < 100 MeV/n
 ULYSSES-HET (nuclei) < 100 MeV/n
 ULYSSES-KET (electrons) < 10 GeV
 CRRES/ONR < (nuclei) 600 MeV/n
 HEAO3-C2 (nuclei) < 40 GeV/n

Short missions (days)/ Larger payloads



CRN on Challenger
 (3.5 days 1985)

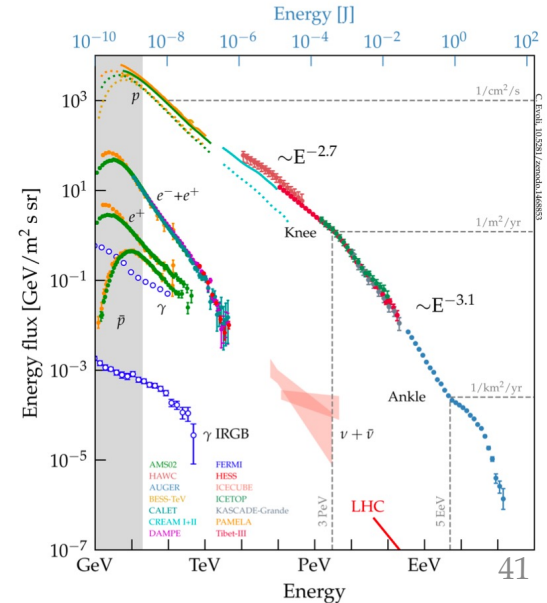


AMS-01 on Discovery
 (8 days, 1998)

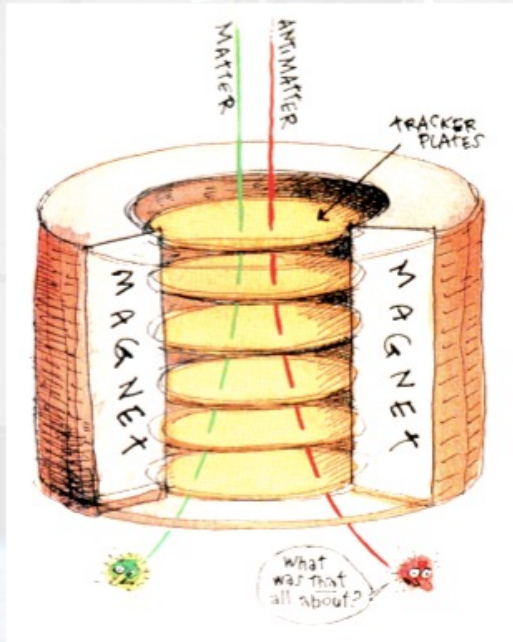


Long missions
Large payloads

Access to space with **long duration missions** allows **direct measurements of CRs** before the interaction with atmosphere. Limited acceptance prevents investigation at highest energies but allows **measurement of CR spectra and composition**



Trackers for cosmic ray measurements



Magnetic Spectrometer

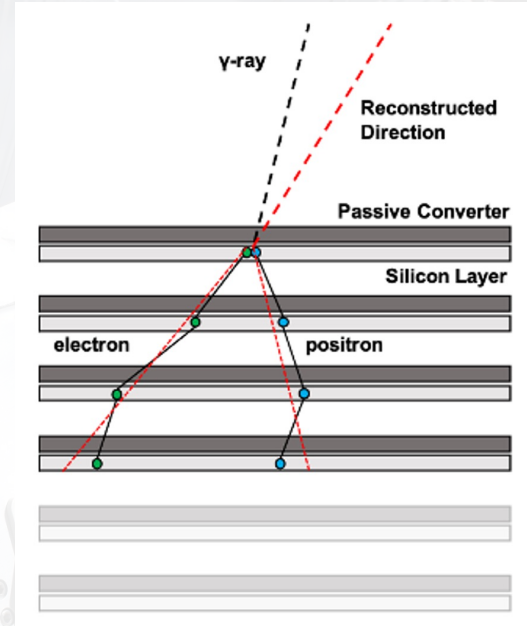
Matter-Antimatter separation

Rigidity measurement

Nuclei Z measurement

Direction reconstruction

(e.g. PAMELA, AMS-02)



Converter Tracker

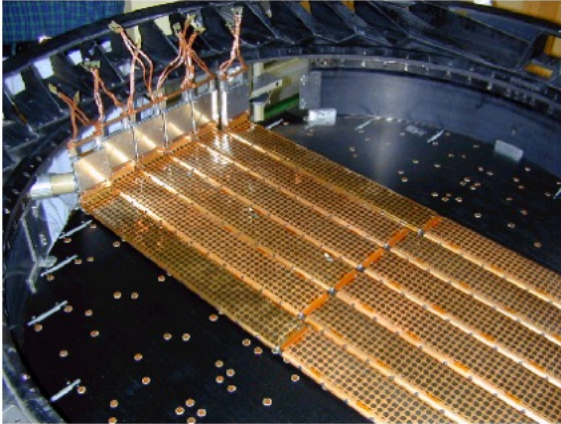
Photon vertex reconstruction

Nuclei Z measurement

Direction reconstruction

(e.g.: Fermi-LAT, DAMPE)

AMS-01 Silicon Tracker



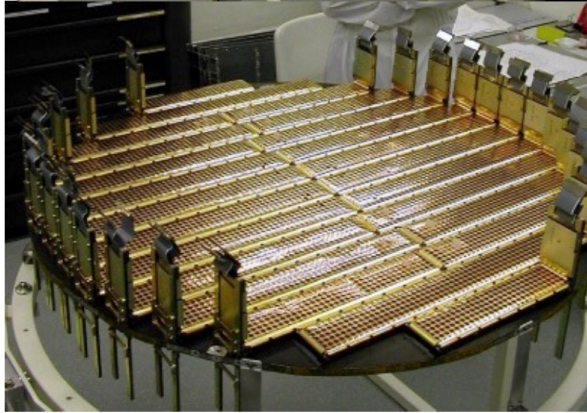
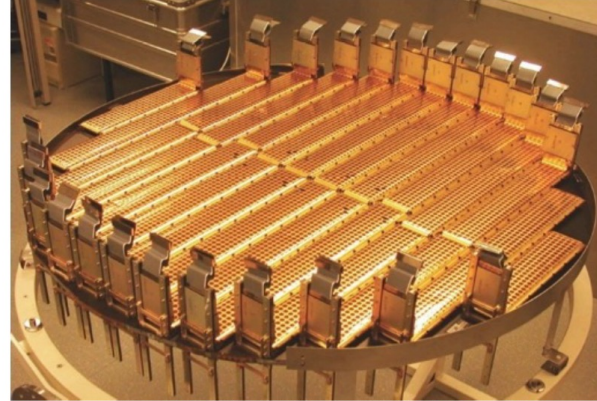
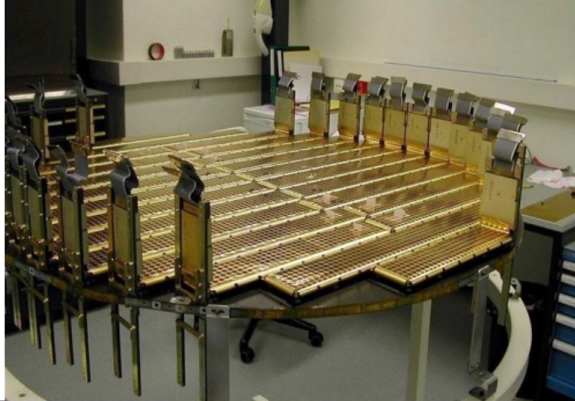
Lightweight carbon fiber shell to hold the planes

- ✓ **Aluminum honeycomb + carbon fiber reinforcement planes**
- ✓ **Front end electronics disposed vertically on the edge of the plane to save acceptance**
- ✓ **Thermal bars to dissipate the power on the magnet mass outside**

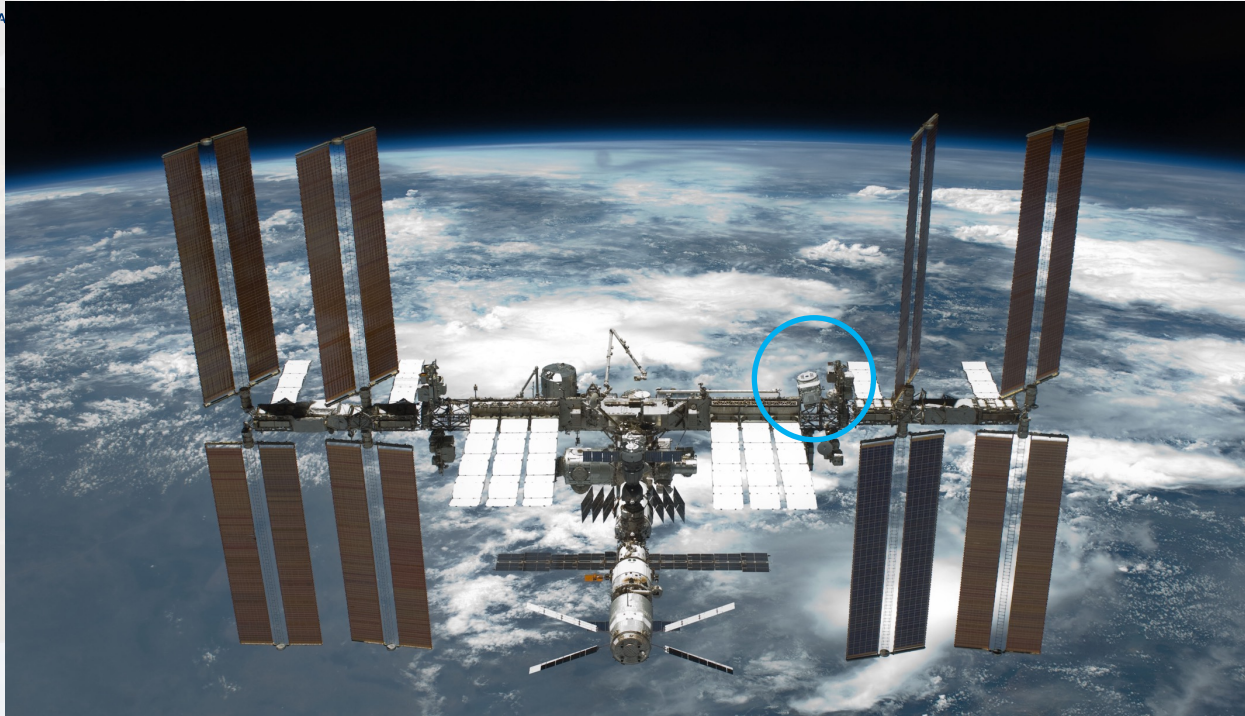


First verification of silicon tracker spectrometer in space (1998)

AMS-02 Silicon Tracker



AMS-02 on the ISS



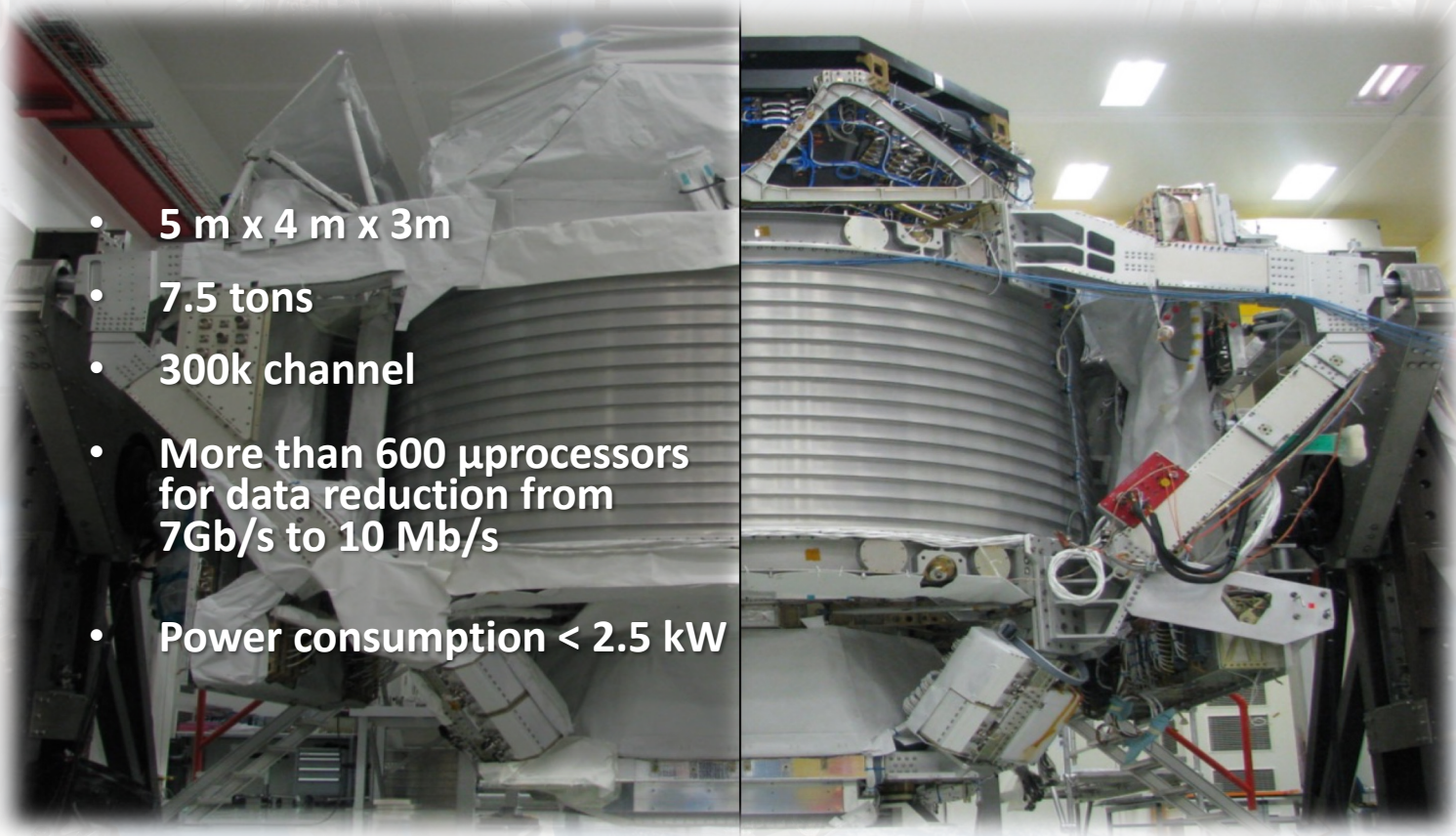
**DIRECT MEASUREMENT OF COSMIC RAYS IN SPACE
ONBOARD ISS SINCE 2011**



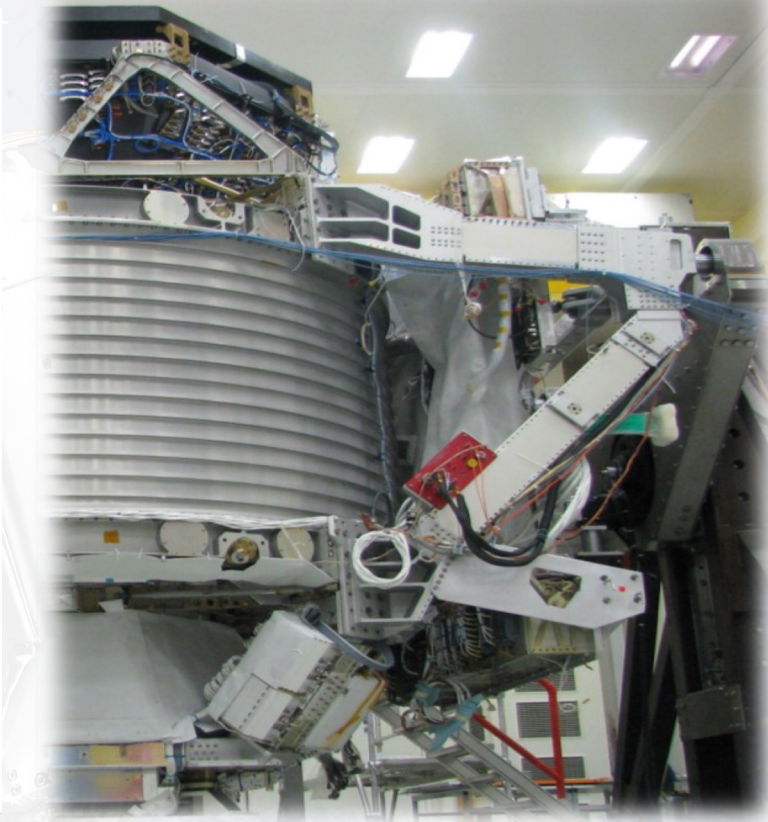
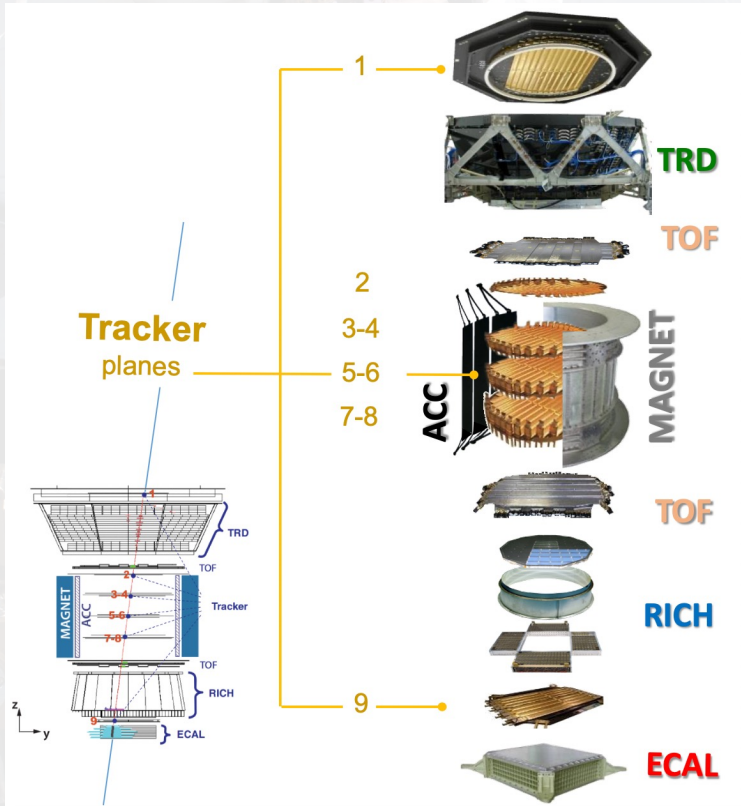
**Cosmic ray antimatter
Indirect search for DM
Spectra and composition
of cosmic rays
Solar Physics**

The AMS-02 detector

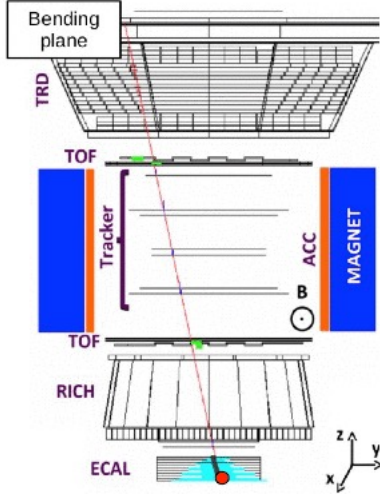
- 5 m x 4 m x 3m
- 7.5 tons
- 300k channel
- More than 600 μ processors for data reduction from 7Gb/s to 10 Mb/s
- Power consumption < 2.5 kW



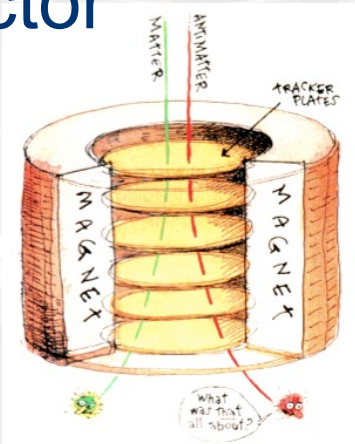
The AMS-02 detector



The AMS-02 detector



	e^-	p	He	
TRD 20 layers				e/p separation charge ($ Z $)
TOF 4 layers				trigger velocity (β) charge ($ Z $)
TRK 9 layers				momentum (p) sign ($\pm Q$) charge ($ Z $)
RICH				velocity (β) charge ($ Z $)
ECAL 20 layers				e^+ energy e/h separation y trigger

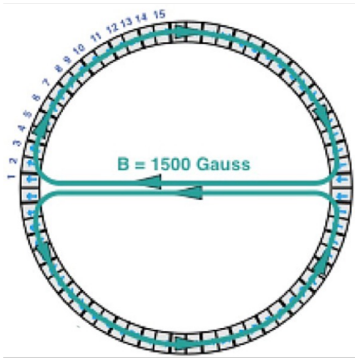


	e^-	P	Fe	e^+	\bar{P}	\bar{He}
TRD						
TOF						
Tracker + Magnet						
RICH						
ECAL						

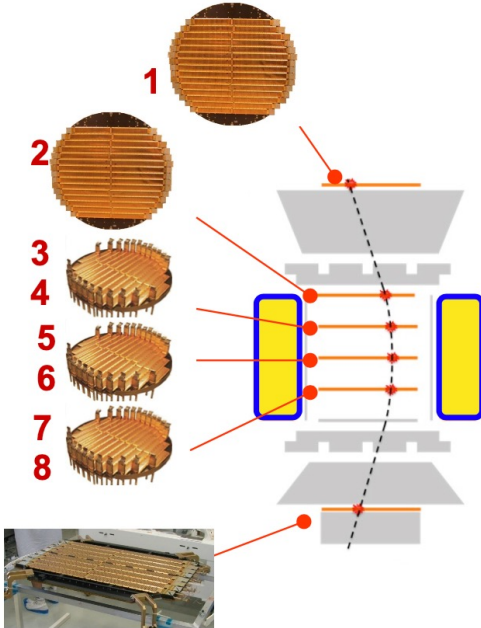
The AMS-02 tracker

9 layers of double sided silicon microstrip detectors inside a 0.14T dipolar magnetic field

192 ladders
2598 sensors
200k readout channels

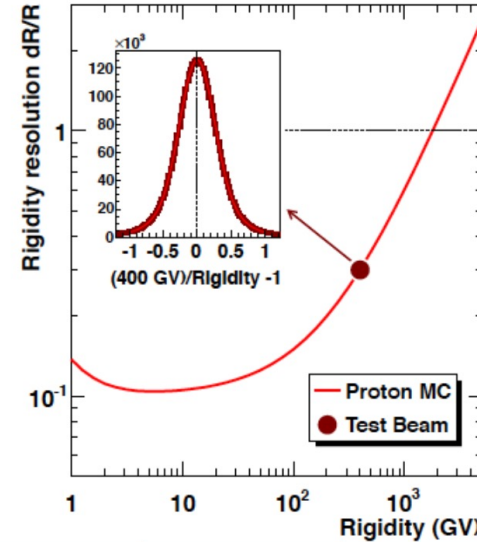


9



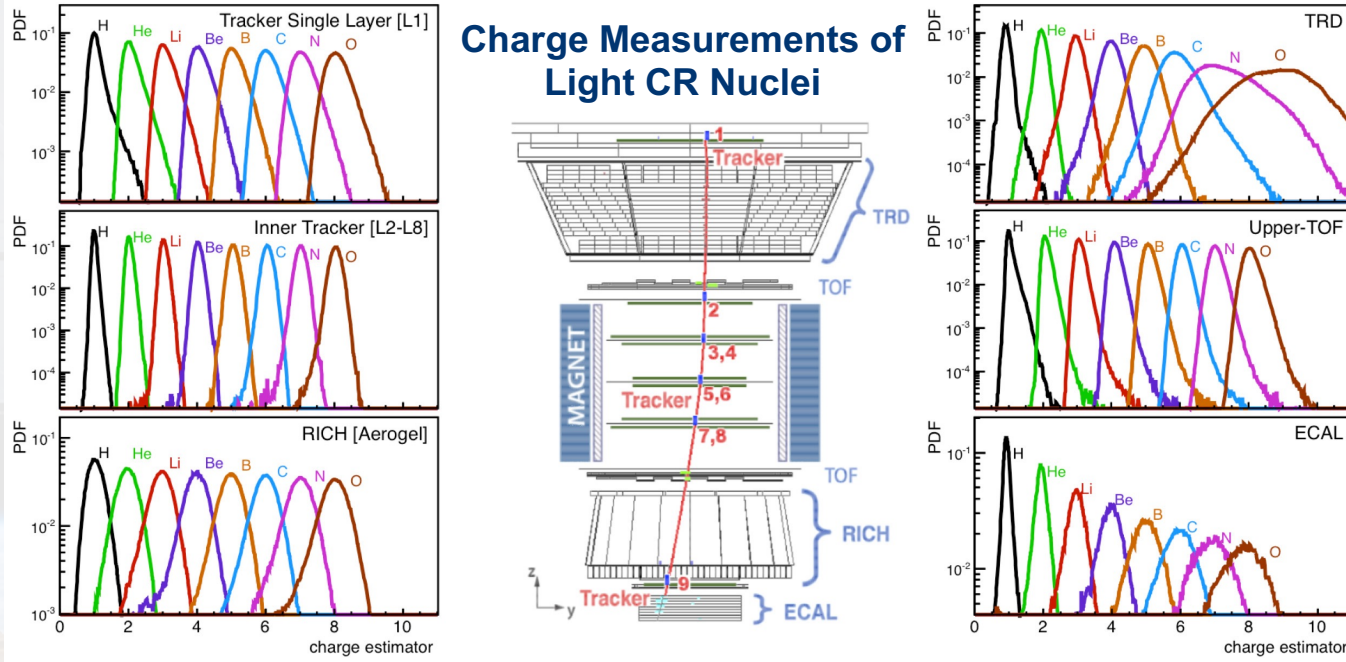
BENDING COO
strip pitch: 27.5 μm
readout pitch: 110 μm

NON-BENDING COO
strip pitch: 104 μm
readout pitch: 208 μm



Charge	Coordinate Resolution	MDR
Z = 1	10 μm	2 TV
2 \leq Z \leq 8	5 - 7 μm	3.2 - 3.7 TV
9 \leq Z \leq 16	6 - 8 μm	3 - 3.5 TV

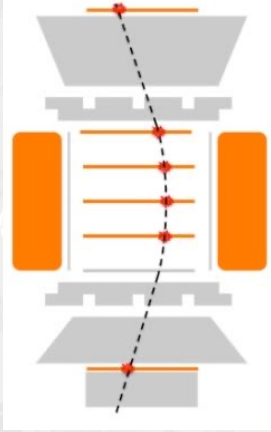
The AMS-02 tracker performances



Redundant measurements of the nuclear charge at different depths of the detector.

Precise understanding of nuclear fragmentation in the materials.

The AMS-02 tracker alignment

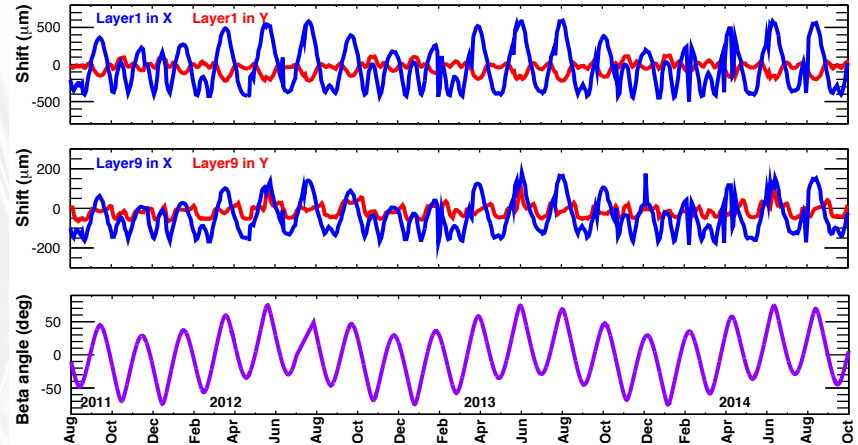


Inner tracker (layers 2 to 8) is arranged in a stiff and lightweight carbon shell and cooled by a mechanically pumped CO₂ bi-phase system

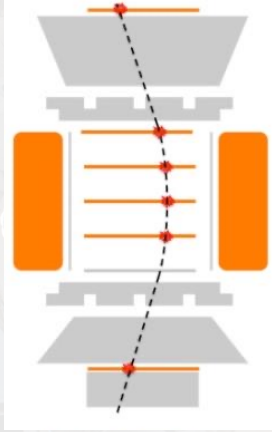
- Thermally and mechanically stable within few mm, relative displacements are continuously monitored by 20 laser beams from layer 2 downwards.

External layers (1,9) are mechanically linked to TRD, ECAL and are affected by thermal movements of the structure

Seasonal effects of the space environment on tracker



The AMS-02 tracker alignment



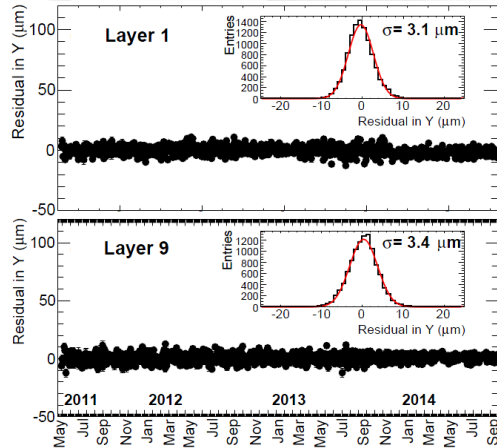
Inner tracker (layers 2 to 8) is arranged in a stiff and lightweight carbon shell and cooled by a mechanically pumped CO₂ bi-phase system

- Thermally and mechanically stable within few mm, relative displacements are continuously monitored by 20 laser beams from layer 2 downwards.

External layers (1,9) are mechanically linked to TRD, ECAL and are affected by thermal movements of the structure

Seasonal effects of the space environment on tracker

Monitor of external layers with CR by means of the study of **Residuals** distance from extrapolated track as reconstructed with the other layers and hit on the layer under study



AMS-02 Reloaded

Tracker Thermal Control System initially developed for 3-year operations.

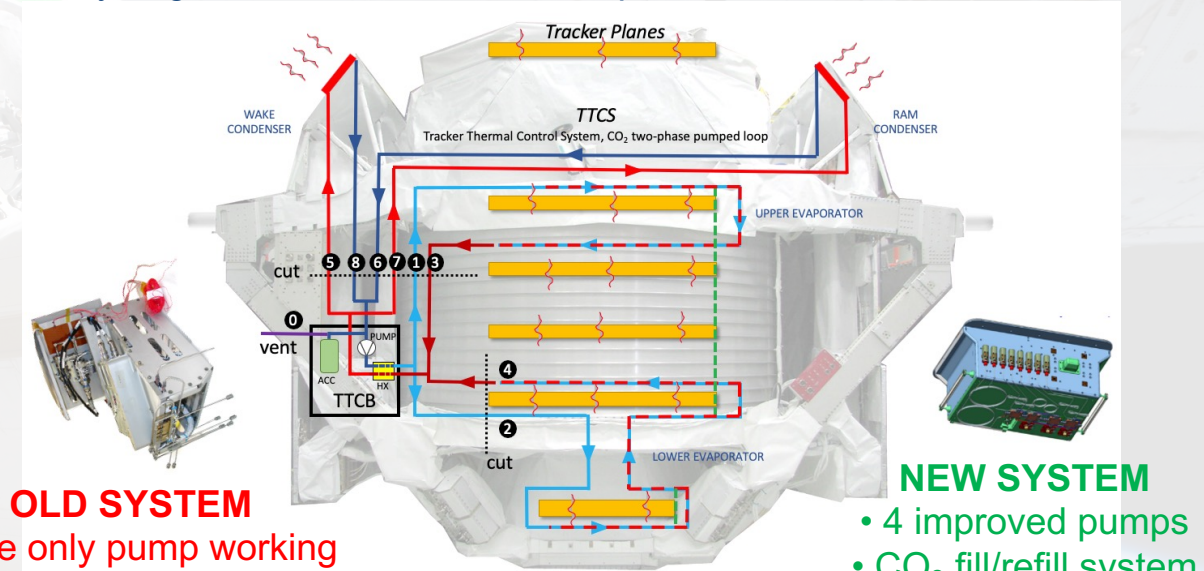
First evidence of defective behavior of the TTCS pumps in 2014.

After 8 years, no more redundancy to guarantee the continuous operations of AMS-02

2014: Start of the **UTTPS** program (Upgrade Tracker Thermal Pump System) in collaboration with NASA.

Replacement of the old TTCS box with **new upgraded system**

The intervention requires a set of **EVA with operations outside ISS** involving cutting and handling of 8 gas tubes



OLD SYSTEM

- One only pump working
- Not enough CO₂ left on last loop
- No pump health monitor

NEW SYSTEM

- 4 improved pumps
- CO₂ fill/refill system
- Additional sensors for pump monitoring

AMS-02 not developed to be upgraded --> one of the most challenging EVA operations in the last decade

The EVA in pills

2019/11/15

- Removal of AMS debris shield
- Toolboxes for next EVAs
- Installation of 6 handrails
- Removal of MLI and VSB structure to facilitate the access to gas tubes

2019/11/22

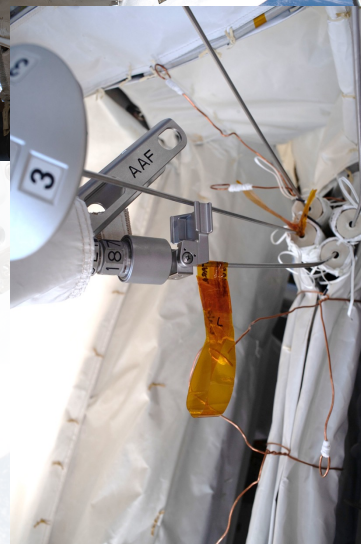
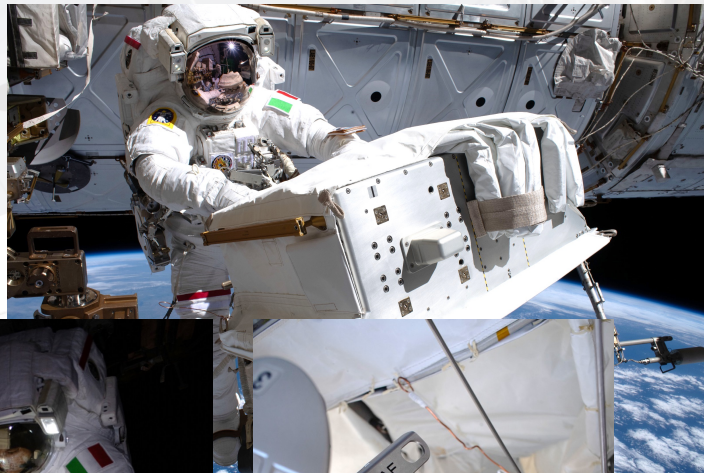
- Rough cut of 2 tubes to release CO2 in space
- Rough cut of 6 additional tubes
- Installation of protection/identification caps

2019/12/03

- Transport of UTTPS and installation on AMS-02
- Connection of power and data cables

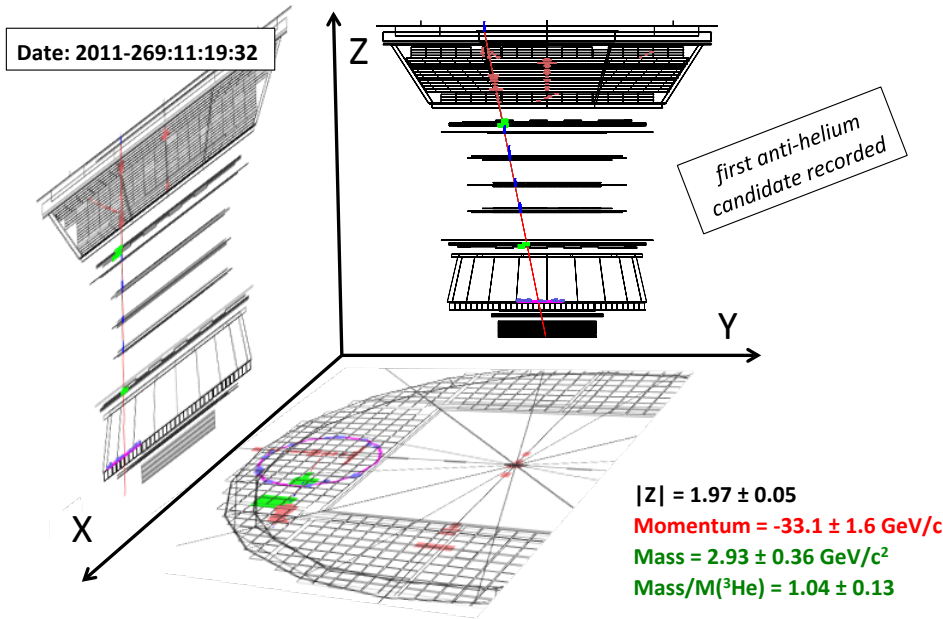
2020/01/25

- Optical leak check
- Cover AMS with MLI



Anti-Helium candidates in AMS-02

Anti-helium is a “golden”-channel, there is no p, K, π contamination, $|Z|$ is well separated, and rigidity resolution is better than $|Z|=1$ particles (MDR = 3.2 TV).



S. J. Ting, AMS collab.
AMS Days 2018

Status of the AMS complex antimatter analysis

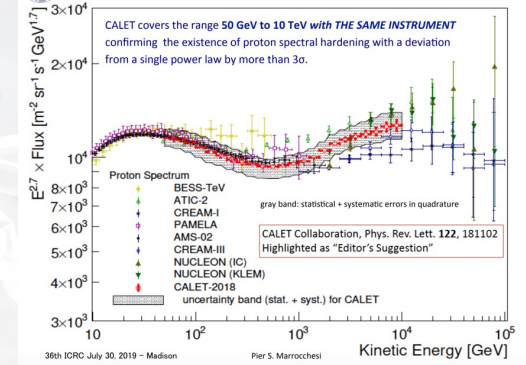
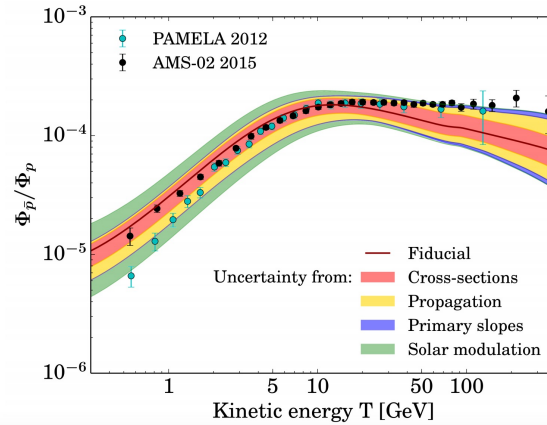
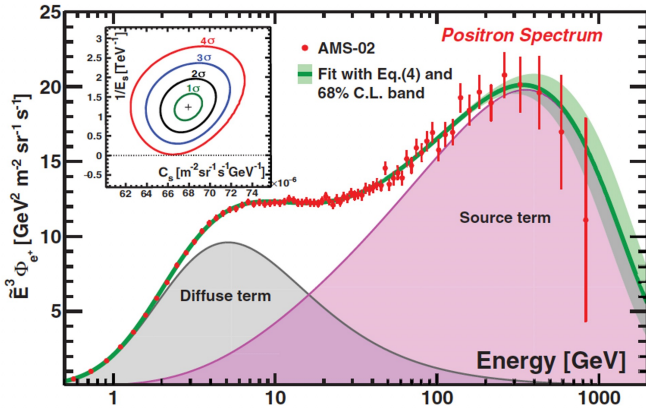
To date we have observed eight $Z = -2$ events with mass around He.

The corresponding sample with $Z = +2$ amounts to one billion helium events.

With the anti-Helium to Helium ratio of less than 1 in 100 million, detailed understanding of the instrument is required.

We are performing final detector verifications before announcing the results

Challenges for next-generation



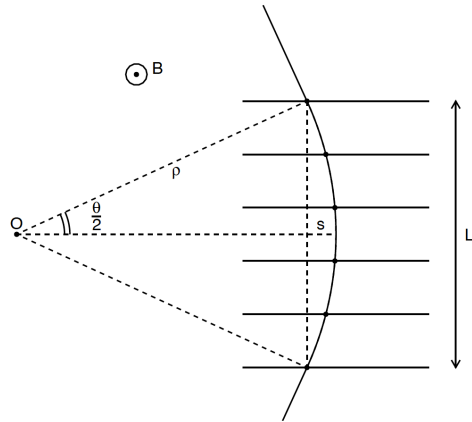
- Electron and positron spectra above 1 TeV
- Cosmic ray composition up to PeV
- Precise determination of low energy abundances and time dependencies
- Search for rare antimatter components (anti-D, anti-He, ...)

.....

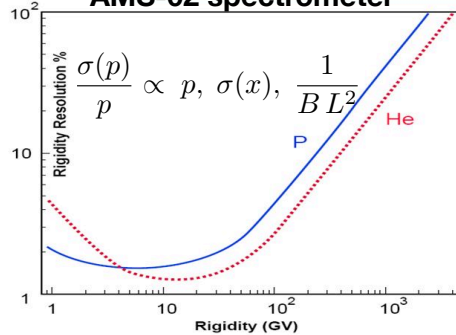
Experimental requirements:
Increased detector acceptance
Improved detector technology
Novel layouts and idea

Challenges for next-generation

Magnetic Spectrometers

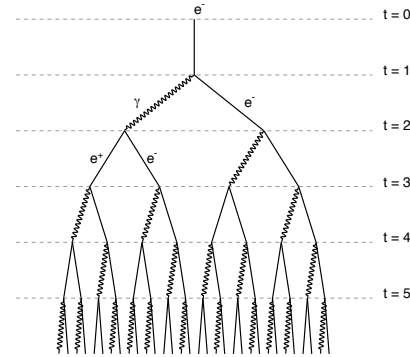


AMS-02 spectrometer

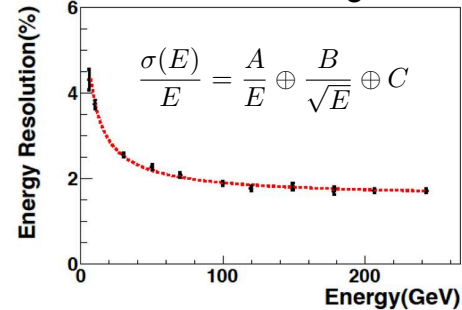


Spectrometer:
energy reach limited by MDR

Calorimeters



AMS-02 electromagnetic calorimeter



Calorimeter:
energy reach limited by statistics

Silicon μ strip detectors in space

Most of space detectors for charged cosmic ray and γ -ray measurements **require solid state tracking systems** based on Si-microstrip (SiMS) sensors.

SiMS detectors are the only solution to instrument large area detectors with larger number of electronics channels coping with the limitations on power consumption in space



Operating Missions						
	Mission Start	Si-sensor area	Strip-length	Readout channels	Readout pitch	Spatial resolution
Fermi-LAT	2008	$\sim 74 \text{ m}^2$	38 cm	$\sim 880 \cdot 10^3$	228 μm	$\sim 66 \mu\text{m}$
AMS-02	2011	$\sim 7 \text{ m}^2$	29–62 cm	$\sim 200 \cdot 10^3$	110 μm	$\sim 7 \mu\text{m}$
DAMPE	2015	$\sim 7 \text{ m}^2$	38 cm	$\sim 70 \cdot 10^3$	242 μm	$\sim 40 \mu\text{m}$

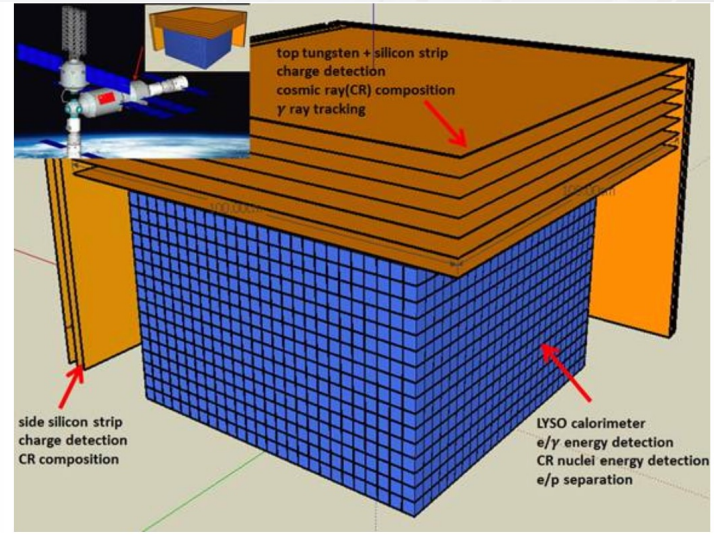
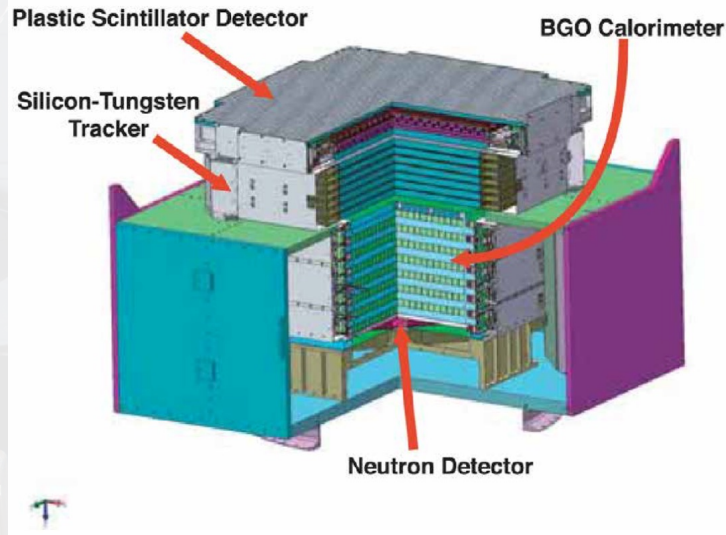
Future Missions						
	Planned operations	Si-sensor area	Strip-length	Readout channels	Readout pitch	Spatial resolution
HERD	2030	$\sim 35 \text{ m}^2$	48–67 cm	$\sim 350 \cdot 10^3$	$\sim 242 \mu\text{m}$	$\sim 40 \mu\text{m}$
ALADInO	2050	$\sim 80\text{-}100 \text{ m}^2$	19–67 cm	$\sim 2.5 \cdot 10^6$	$\sim 100 \mu\text{m}$	$\sim 5 \mu\text{m}$
AMS-100	2050	$\sim 180\text{-}200 \text{ m}^2$	$\sim 100 \text{ cm}$	$\sim 8 \cdot 10^6$	$\sim 100 \mu\text{m}$	$\sim 5 \mu\text{m}$

[1] HERD Collaboration. *HERD Proposal*, 2018 <https://indico.ihep.ac.cn/event/8164/material/1/0.pdf>

[2] Battiston, R.; Bertucci, B.; et al. *High precision particle astrophysics as a new window on the universe with an Antimatter Large Acceptance Detector In Orbit (ALADInO)*. Experimental Astronomy 2021. <https://doi.org/10.1007/s10686-021-09708-w>

[3] Schael, S.; et al. *AMS-100: The next generation magnetic spectrometer in space – An international science platform for physics and astrophysics at Lagrange point 2*. NIM-A 2019, 944, 162561. <https://doi.org/10.1016/j.nima.2019.162561>

Next generation calorimeter mission: HERD



This generation (DAMPE, CALET, AMS-02, ...): only CRs from top are detected
Next generation: "**Calocube**" approach: develop a calorimeter that is sensitive also to particles from the side
--> increase statistics without increasing volume and weight

Next generation calorimeter mission: HERD

Scientific goals:

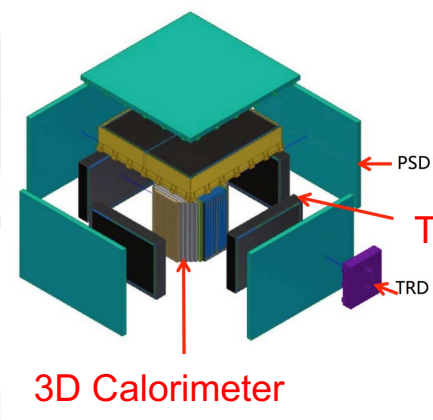
- search of dark matter signatures
- investigate origin of cosmic rays
- study of the highest energy particles

Key features:

- acceptance 10-20 times than existing experiments
- weight limited to fit space constraints

R&D activity to define the best layout of the detector:

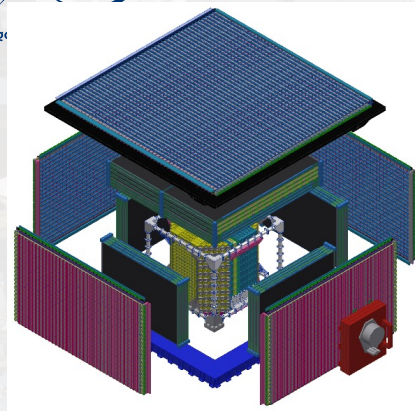
- Silicon tracker and Sci-Fi tracker
- Si-based charge detector
- Calorimeter layout optimization
- Deployment of novel detectors in space (SiPM)
- Mechanical structure
-



3D Calorimeter



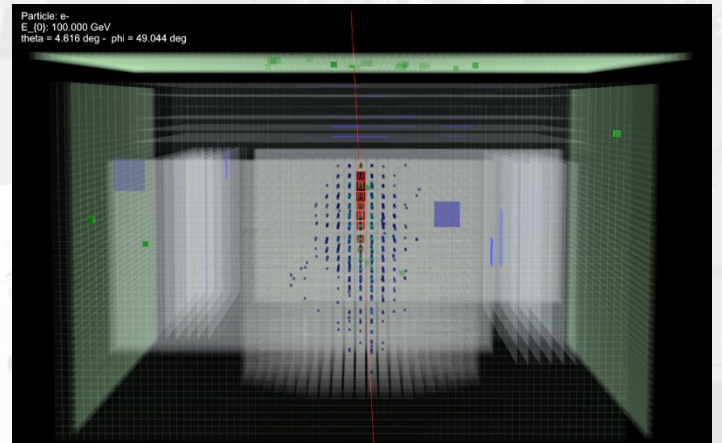
Next generation calorimeter mission: HERD



PSD
Gamma identification
Charge measurement

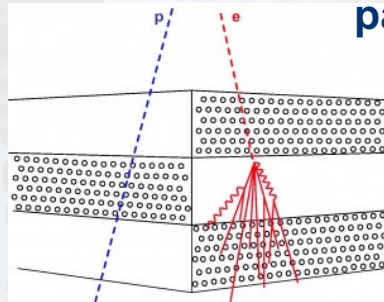
Tracker
Charge measurement
CR trajectory
Gamma converting & tracking

TRD
TeV CR calibration

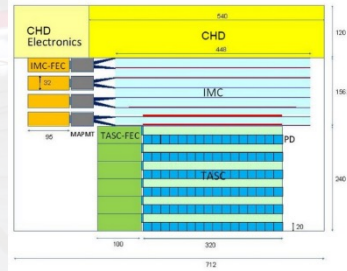


CALO: 3-d imaging calorimeter: Energy measurement & Particle identification

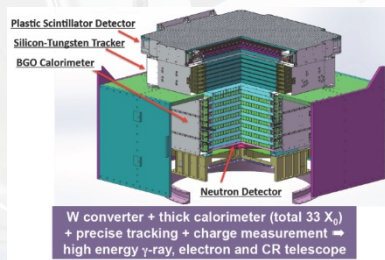
The novel design of 3-d imaging calorimeter could significantly increase GF, improve particle discrimination and reduce systemic error



AMS-02



CALET



W converter + thick calorimeter (total 33 X₀)
+ precise tracking + charge measurement →
high energy γ-ray, electron and CR telescope

DAMPE

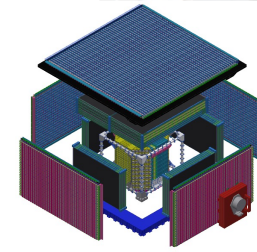
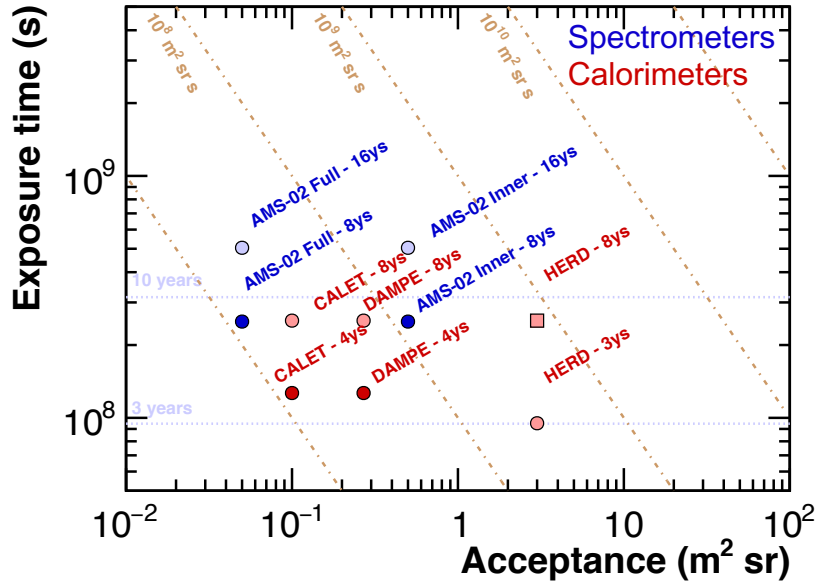
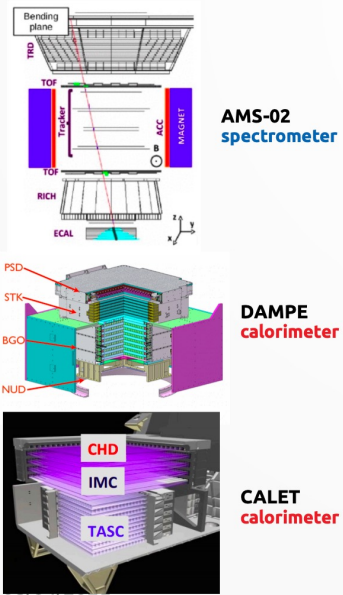


HERD

The future of magnetic spectrometers

HERD will be the workhorse cosmic ray observatory in space in 2030.

However, without a spectrometer, the legacy of AMS-02 for antimatter physics in space will not be continued.



**HERD
calorimeter**

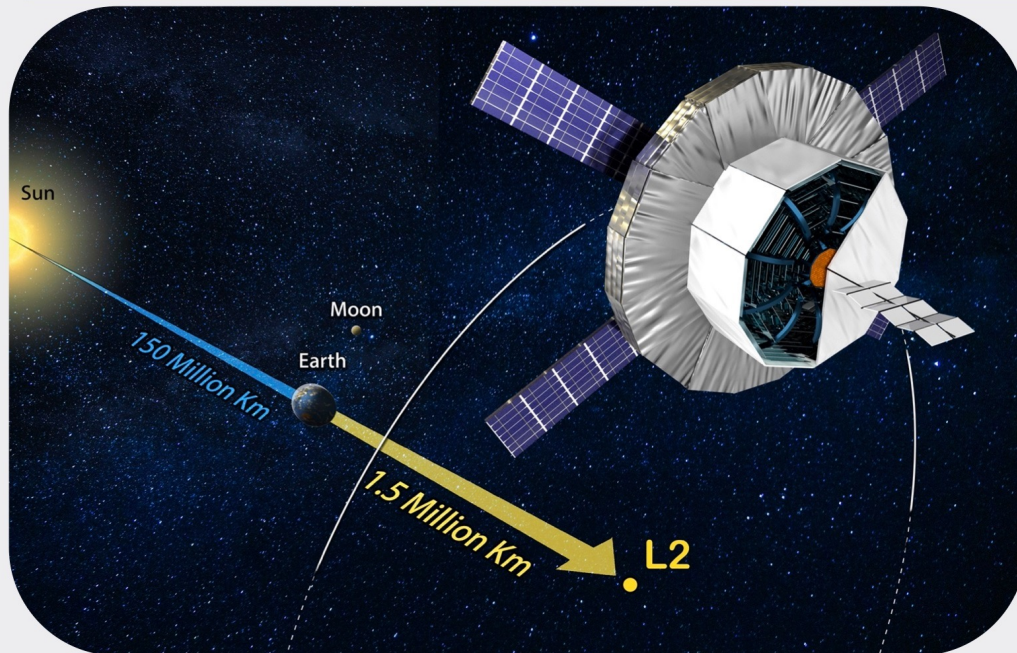
AMS is the only magnetic spectrometer that is (so far) planned to be operated in space

Next-gen spectrometer mission: ALADInO

<https://doi.org/10.3390/instruments6020019>

Progressing in particle astrophysics with the
Antimatter Large Acceptance Detector In Orbit

ALADInO



**High Temperature Superconducting
Magnetic Spectrometer in space**

Acceptance $> 10 \text{ m}^2\text{sr}$
Antimatter measurements up to 10 TeV
Established technologies for detection of
particles in space

5-year operations in L2

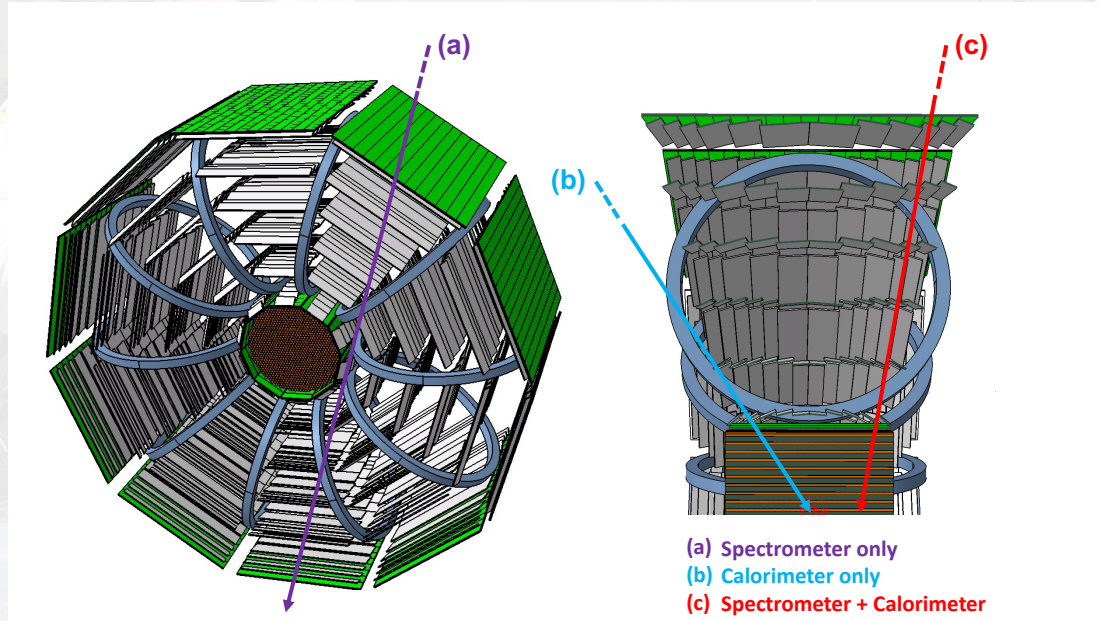
Payload Weight $< 6.5 \text{ t}$
Payload power consumption 3 kW
Compact volume (fits Ariane launcher)

Roadmap for mission opportunity

mid 2030s: ALADInO Pathfinder
mid 2040s: Operations in L2
by 2050: Unprecedented results

Next-gen spectrometer mission: ALADInO

An Antimatter Large Acceptance Detector in Orbit



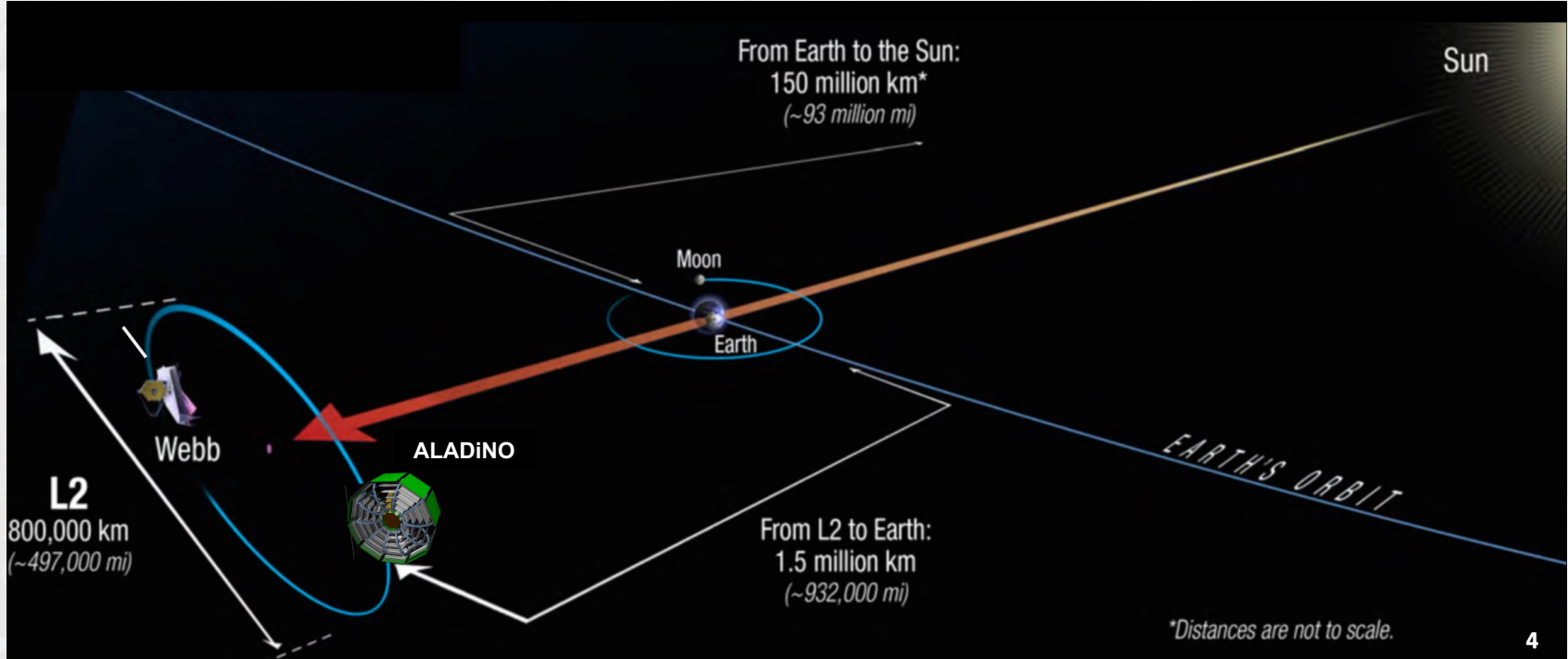
High Temperature Superconducting (HTS) magnetic spectrometer (SMS) to measure the particle rigidity, charge magnitude and sign with $MDR > 20 \text{ TV}$ and acceptance $> 10 \text{ m}^2 \text{ sr}$

Time of Flight (ToF) system to measure the particle velocity and charge magnitude;

Large acceptance ($\sim 9 \text{ m}^2 \text{ sr}$) 3D imaging calorimeter (CALO)

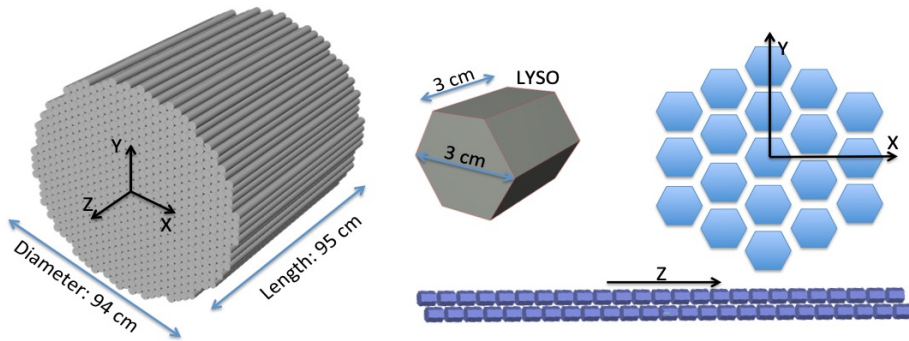
Next-gen spectrometer mission: ALADiNO

The best place to operate a cryogenic superconducting magnet in space is Lagrangian point L2, like the Webb space telescope, to minimize the active cooling of the cryo-magnet



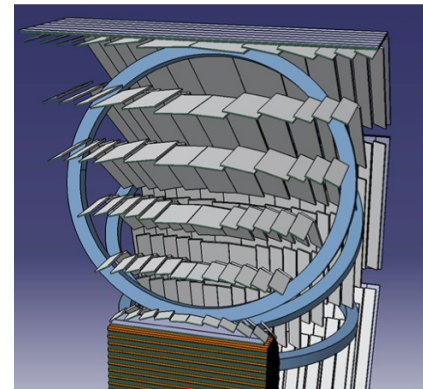
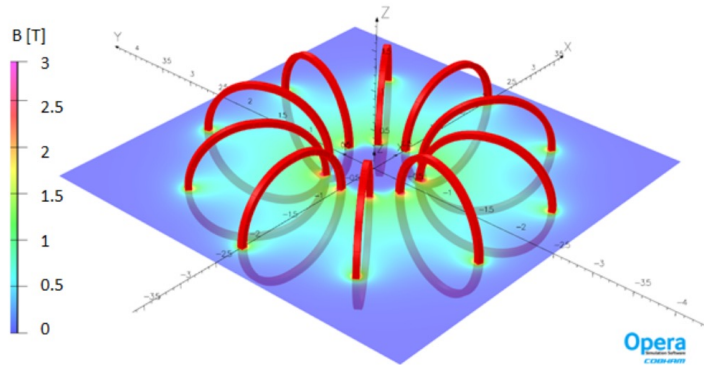
Next-gen spectrometer mission: ALADInO

Agenzi



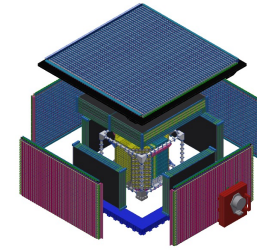
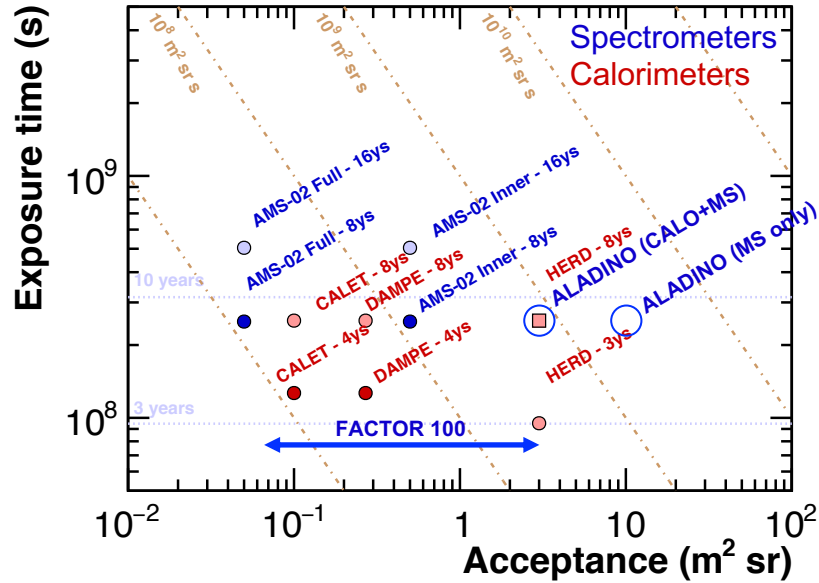
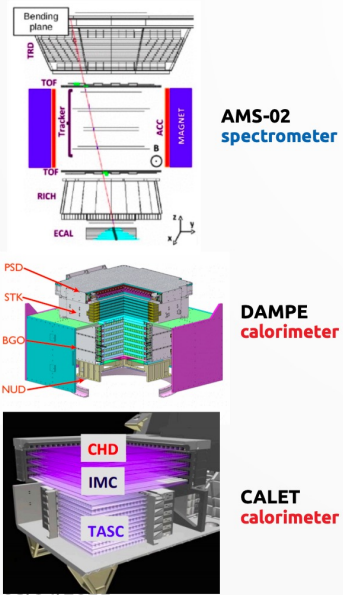
The core: a symmetric LYSO calorimeter with 61 X_0 depth

The spectrometer: 0.8T average field generated by HTS coils and silicon tracker system with optimized geometry

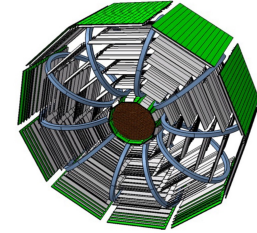


The future of magnetic spectrometers

ALADINO will improve by a factor of 100 the current acceptance of AMS-02



HERD
calorimeter

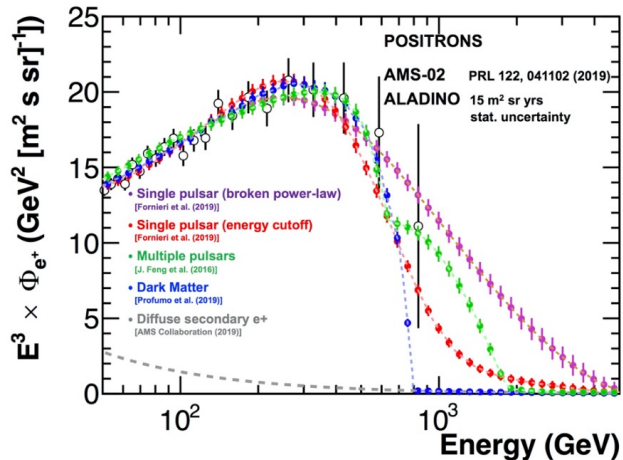


ALADINO
spectrometer

Next-gen spectrometer mission: ALADInO

Agenzia Spaziale Italiana

ALADINO will extend the physics of HERD including the capability to separate matter/antimatter CR in the TeV energy range (which is the current limit of the AMS-02 spectrometer in operation)



Positron and electron spectra at energies > 1TeV will provide unique information to understand the origin of the positron excess observed by AMS-02

Heavy anti-matter CRs (anti-D, anti-He) will be in reach to be measured by ALADInO

